12-13-2002

Development of Application Program for Harmonic Analysis

Sunitha Uppalapati

DEVELOPMENT OF APPLICATION PROGRAM FOR HARMONIC ANALYSIS

By

Sunitha Uppalapati

A Thesis
Submitted to the Faculty of
Mississippi State University
in Partial Fulfillment of the Requirements
for the Degree of Master of Science
in Electrical Engineering
in the Department of Electrical and Computer Engineering

Mississippi State, Mississippi

December 2002

DEVELOPMENT OF APPLICATION PROGRAM FOR HARMONIC ANALYSIS

By

Sunitha Uppalapati

Approved:

S. Mark Halpin
Professor of Electrical and
Computer Engineering
(Major Advisor and Director
of Thesis)

Stanislaw Grzybowski
Professor of Electrical and
Computer Engineering
(Committee Member)

Nicholas H. Younan
Professor of Electrical and
Computer Engineering (Graduate
Coordinator)

Michael S. Mazzola
Associate Professor of Electrical
and Computer Engineering
(Committee Member)

A. Wayne Bennett
Dean of the College of Engineering

Name: Sunitha Uppalapati

Date of Degree: December 13, 2002

Institution: Mississippi State University

Major Field: Electrical Engineering

Major Professor: Dr. S. Mark Halpin

Title of Study: DEVELOPMENT OF APPLICATION PROGRAM FOR HARMONIC ANALYSIS

Pages in Study: 94

Candidate for Degree of Master of Science

Increased power quality problems due to intensive usage of power electronic devices resulted in development of software applications to perform quick harmonic analysis. However, the present harmonic analysis applications have special software or computer locks requirements and occupy huge memory and cost high. An application program (using Microsoft Visual C++) that is simple yet accurate in calculations; with no special software or high memory requirements is developed in this thesis work. The program uses the automatic acceptance criteria (AAC) and the harmonic penetration techniques in calculating the system voltages. Several user-friendly features and tools that aid in better understanding of system harmonics are included in the program. Comparison of case study results with Superharm simulation results proves the program's accuracy. This thesis work resulted in an informative and time saving program with which the user can document the study results and analyze them with minimum effort.

DEDICATION

Ma – to you.

ACKNOWLEDGEMENTS

I would like to primarily thank Dr. S. Mark Halpin, my research advisor and major professor, for giving me the opportunity to be one of his research students and for his expert guidance throughout my Masters program. I would also like to thank Dr. Grzybowski and Dr. Mazzola for their valuable time and suggestions. I would like to thank all the persons who helped me through my student career. I wish to thank my family, with out whose blessings, love and faith I could not have been what I am.

TABLE OF CONTENTS

CHAPTER | Page

LIST OF TABLES

TABLE Page

LIST OF FIGURES

FIGURE Page

FIGURE Page

FIGURE Page

CHAPTER I

INTRODUCTION

Nonlinear devices such as the switch mode power supply, adjustable speed drives, etc. cause harmonic problems in power systems. The efficiency of such devices largely depends on the quality of power supplied. Nonlinear loads produce harmonic currents, which in turn distort the supply voltage waveform. Excessive harmonic currents can lead to serious problems such as overheated wires and transformers, increased energy costs, and system degradation and failure which can result in revenue loss to the utility. In order to control harmonics, IEEE Standard 519, "Recommended Practices and Requirements for Harmonic Control in Electrical Power Systems," was adopted. IEEE 519 outlines limitations on voltage and current harmonics in order to ensure that harmonic distortion levels throughout the entire electrical distribution system, from utility to consumer, will remain low enough for the system to function properly.

IEEE Standard 519 suggests limitations for voltage and current harmonic contaminations. The standard sets the limits as a divided responsibility between utility and customers as follows:

A. The customer: IEEE 519 considers the "point of common coupling (PCC)" as the customer-utility interface point. With end-user equipment being mostly the source of harmonics, the standard limits the amount of harmonic currents injected by the end-user loads. Harmonic current limitations for the end user apply at the PCC.

B. The utility: The utility system is the entity consisting of the transmission system and/or the distribution system that serves the end-user (customer or industry plant). The utility has control over the system impedance that is responsible for the voltage distortion at the point of common coupling. For most utility systems, the IEEE 519 Standard requires the total harmonic distortion of the voltage to be less than 5% at the PCC. This implies that the utility is responsible to insure that the system conditions do not result in unacceptable voltage distortion levels if all customers are within the recommended guidelines for harmonic current generation at their PCC.

IEEE 519 harmonic current limits are specified in terms of the short circuit current and the maximum load demand current. IEEE 519 compliance evaluation requires values of the short circuit current and the maximum load current. However, IEEE 519 (harmonic current) standard compliance can also be estimated using a simple automatic acceptance criteria (AAC) that can be used to avoid the detailed study for evaluating the IEEE 519 compliance.

IEEE 519 sets current distortion limits such that voltage distortion limits are not exceeded assuming a reasonable supply impedance. Conceptually, if the currents injected by nonlinear loads satisfy IEEE 519 current limits then the voltage distortion would also satisfy the IEEE 519 voltage limit in order that no potential harmonic related problem arises. Therefore, as a primary check for any potential harmonic problems, the current distortions caused by the nonlinear loads must be checked for IEEE 519 compliance.

Depending on whether or not the harmonic currents of the nonlinear loads exceed the limits based on a simple evaluation, a detailed study of the harmonic problem can be conducted. If the harmonic currents exceed the limits a detailed study of the harmonic problem is conducted: otherwise a detailed study is not necessary. This saves the computational effort of an unnecessary detailed study and time for making any engineering decisions. Therefore, if the simple AAC estimation results in high levels of harmonic currents, then voltage distortions may be found to analyze the comprehensive effect of harmonics on the power system. Given the estimated system response (system harmonic voltages), preventive measures can be taken to avoid any potential equipment damage due to harmonics. Such comprehensive harmonic analyses are frequently required for proper operation of electrical equipment. To shorten the amount of time in estimating the harmonic effects, several software programs have been developed by software vendors for both utility and industrial power system analysis.

Engineers and software developers have been continuously improving software for power system applications. The user-friendly features of the Microsoft Windows operating system made it possible to build new software applications that are convenient to use. The improved applications help the user to get a better idea of the severity of harmonics. A software application that estimates the harmonic effect on a power system due to nonlinear load harmonic currents has been developed in this thesis work.

To validate the accuracy of the application program developed, case studies were run using the application program developed and the results were compared with the Superharm simulated results for the same case. The comparison proves that the application program developed generates accurate results. However, the accuracy of the application is relative to Superharm. Therefore the applicability of the program to any power system is dependent on the assumptions and any in-built errors of Superharm as described in the Superharm's application benchmarking guide [1].

Scope of Thesis

A software application using the Microsoft Foundation Classes (MFC) and the Microsoft Visual C++ language was developed on the Windows platform. The emphasis was on the user interface features of the application to make the application as user friendly as possible. The application has both numerical and graphical data representation using some of the advanced features of Microsoft Visual C++. The visual display of distorted harmonic waveforms (current and voltage) available in the application gives the user a better understanding of the harmonics in their power system. The application uses an AAC method to estimate the severity of current harmonics with respect to the IEEE 519 standard and the current injection method is used to find the system response. The theoretical concepts used and the work done to develop the application is discussed in this thesis document.

CHAPTER II

THE ANALYTICAL APPROACH

Introduction

A software program that estimates the compliance of a utility's customers with IEEE 519 current limits is developed in this thesis work. The analytical logic behind the software program is discussed in this chapter. The analytical logic for the software program is developed for a sample power system network consisting of the most generally found equipment in a real life power system network. The system has a transformer, two shunt capacitors, two cables or lines, a supply source and nonlinear loads. Some of the most commonly found nonlinear loads are provided for ease of use.

Nonlinear loads at customer sites inject harmonic currents onto the distribution system. The distorted harmonic currents cause distorted voltage drop. Therefore, the harmonic analysis study in this application program consists of two major parts. The first part is estimating harmonic current compliance with the IEEE 519 limits. The second is finding harmonic voltages throughout the system. The following methods are used to in the program.

1) An automatic acceptance criteria is used for estimating the IEEE 519 harmonic current limit compliance.
2) A current injection method is used for estimating the bus voltages.

The Automatic Acceptance Criteria

The automatic acceptance criteria (AAC) is a conservative approach for estimating IEEE 519 compliance for harmonic currents injected by nonlinear loads. Weighting factors (W_i) that are numerical values signifying the severity of the harmonic distortion caused by different loads are used in this method. Nonlinear loads with high total harmonic distortion THD factors have high weighting factors. For example, consider a single-phase power supply load and a 12 pulse converter. The typical current waveform for a single-phase power supply load would be as in Figure 2.1. The single-phase power supply load has a high THD because the harmonic current injected by it deviates more from a pure sinusoidal shape. However, a 12 pulse converter has a typical current waveform such as in Figure 2.2. The waveform in Figure 2.2 deviates (from a pure sine wave) less as compared to the waveform in Figure 2.1. Therefore, the weighting factor for a 12 pulse converter is smaller than that of a single-phase power supply load.

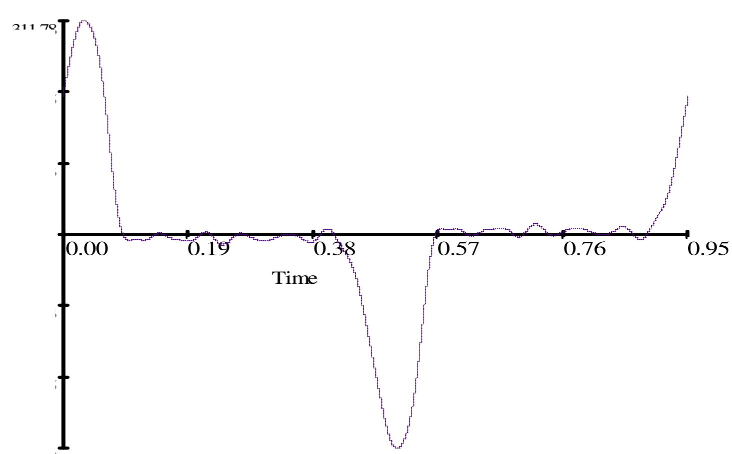

Figure 2.1. Typical Current Waveform for a Single-Phase Power Supply Load.

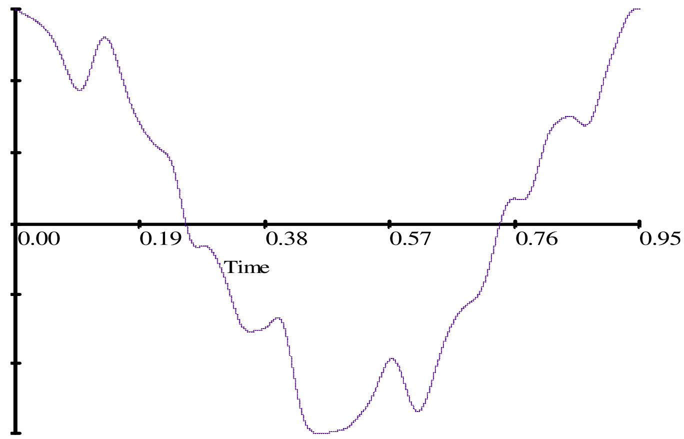

Figure 2.2. Typical Current Waveform for a 12 Pulse Converter Load.

Various common nonlinear loads and their corresponding weighting factors used in the AAC are tabulated in Table 2.1.

Table 2.1. Weighting Factors for Different Loads.

Type of load	**W**
Single-phase Power Supply	2.5
Semi converter	2.5
6 pulse converter capacitive smoothing, no series inductance	2.0
6 pulse converter capacitive smoothing, series inductance >3% or DC drive	1.0
6 pulse converter with large inductor for current smoothing	0.8
12 pulse converter	0.5
AC voltage regulator	0.7
Fluorescent lighting	0.5

The automatic acceptance criteria is applied at the point of common coupling (PCC). To apply the AAC to a set of nonlinear loads in a system they must have a common point of coupling with the distribution network. The AAC method is applied individually to each customer with a common point of coupling. For the system for which the program is designed there is only one common point for all the nonlinear loads. The following steps summarize the application of the automatic acceptance criteria.

1. Determine the short circuit capacity, S_{sc}, at the PCC.
2. Determine the value of S_{Di}, the kVA value of the i^{th} nonlinear load connected to the PCC. If a customer uses two 12-pulse converters of sizes x kVA and y kVA then S_{Di} of the 12-pulse converter type of load is (x+y) kVA. If a new 12-pulse converter nonlinear load is to be added then its kVA value is also added.
3. Evaluate the weighted short circuit power, S_{DW}, at the PCC as in (2.1). The subscript i in (2.1) indicates the i^{th} nonlinear load or group of loads.

$$S_{DW} = \sum_{i} S_{Di} * W_i \tag{2.1}$$

4. The harmonic current produced by the customer load is acceptable if the ratio of weighted short circuit power to the short circuit capacity at the PCC satisfies (2.2). The conservative 0.1% ratio insures that the loads would be in compliance with IEEE 519.

$$\frac{S_{DW}}{S_{SC}} < 0.1\% \tag{2.2}$$

The AAC is a crude approach for estimating if the harmonic currents due to a certain capacity or quantity of the nonlinear loads of Table 2.1 would satisfy the IEEE

519 standard current limits. The IEEE 519 standard sets limits in terms of the ratio of available short circuit current at PCC and maximum demand current. The larger a supply system is relative to a nonlinear load connected to it, the more likely that the system is "safe" in terms of harmonic problems. The AAC uses the same concept only in terms of different quantities. The weighted distorting load power, S_{DW}, represents the level of harmonic currents possibly injected by nonlinear loads under study.

To use the standard method of evaluating IEEE 519 limit compliance, the maximum demand current value is required. For an existing customer, the maximum demand current value can be calculated as an average of measured current values over a period of time. But for new customers, the maximum load demand current should be calculated using anticipated peak operation of the plant [2]. However, the capacity of nonlinear load proposed to be installed and the short circuit capacity of the supply system is all that is needed to get a conservative estimation using AAC method.

The AAC part of the software application can be used in estimating limit compliance when adding a new customer or when installing a new nonlinear load. If the ratio of (2.2) is not satisfied then the system bus voltages could be found. Once the bus voltages are found, the resulting current harmonics flowing through different components of the system can be determined in order to analyze the total harmonic affect on the system.

System Response Estimation

Bus voltages (system response) at each harmonic frequency show the true impact of harmonic sources on a power system. The bus voltages for a given set of nonlinear loads can be found by the harmonic penetration method. The application program discussed here uses the harmonic penetration method to find the system response. The analytical approach used in the application to find the system bus voltages can be divided into the following systematic steps.

1. Get the data required for individual components of the network.
2. Convert these values into per-unit on consistent bases.
3. Build the admittance matrix $[\overline{Y}]$ of the network to represent the network mathematically.
4. At each frequency of interest, form the current injection vector $\tilde{\tilde{I}}$ and find the corresponding harmonic voltages $\tilde{\tilde{V}}$ at different buses.

The systematic steps outlined previously are logically coordinated in the application to do the required manipulations to obtain the desired output (system voltages). The logical sequence and the theoretical justification of the same are explained in the remaining sections of this chapter.

Retrieving the Data for Individual Components

Supply source, transformers, capacitors, cables or lines and loads dominate the power system impedance. The severity of harmonics on a distribution system largely depends on system impedance. The built-in sample system is a simple system topology that represents the vast majority of the distribution systems serving customers (from a harmonic study prospective). Therefore, the system in Figure 2.3, with most of the commonly found electrical distribution system components is considered in this application program. Because manufacturers provide most equipment impedance data in sequence components, sequence networks are used to represent the system. The input data needed by the application is entered through dialog boxes – the part of the application that is a graphical user interface (GUI) is described in Chapter 3. The components and the format of individual input data required by the application are summarized in Table 2.2.

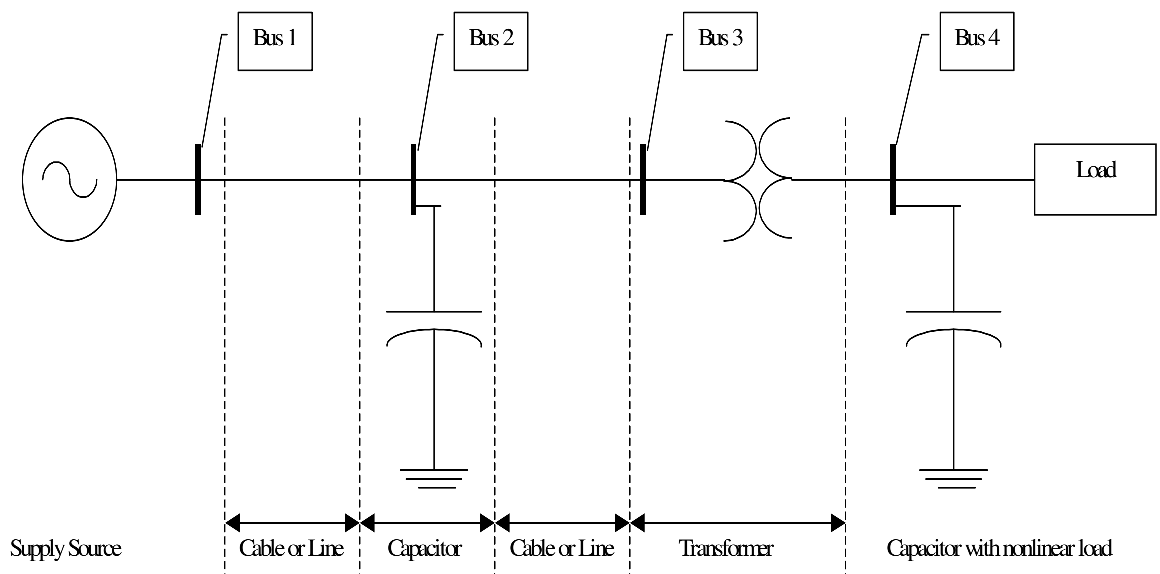

Figure 2.3. Single Line Diagram of the System Used for Study.

Table 2.2. Input Data for Different Components.

Component name	Data Supplied by the User
Supply Source	1. Three phase kVA 2. Phase to phase kV 3. Positive sequence resistance and reactance in per unit based on given kVA and kV values 4. Zero sequence resistance and reactance in per unit based on given kVA and kV values
Cable or Line	1. Phase to phase kV 2. Three phase kVA 3. Positive sequence resistance and reactance in per unit based on given kVA and kV values 4. Zero sequence resistance and reactance in per unit based on the given kVA and kV values
Shunt Capacitor	1. Three phase kVAr 2. Phase to phase kV
Transformer	1. Three phase kVA 2. Phase to phase high voltage kV 3. Phase to phase low voltage kV 4. Percent impedance (%Z) 5. X to R ratio 6. Tap in kV on the HV side. 7. Type of connection (Y-△, △- △ etc) 8. Grounding resistance and reactance on HV and LV sides in ohms.
Load	1. Three phase kVA 2. Phase to phase voltage kV 3. Power factor (displacement factor) 4. Harmonic (h=1 to 50) current magnitudes in percentage of the fundamental and angle in degrees

The last component in Table 2.2 is a nonlinear load. As stated in Table 2.2, the application requires the harmonic current information as part of the input data. The typical harmonic characteristics of several nonlinear loads are available for default use in the application. If measured harmonic data is available and is different from the typical data provided, the user can modify the data and the modified data is used to find the system response. In the absence of measured data, the typical values available in the application can be used for studying the harmonic impact on the system. Most of the harmonic current data for the nonlinear loads that are considered in this thesis were obtained from the case studies in the Superharm manual [3, 4]. For some of the loads, like the 6-pulse converter and the 12-pulse converter, data was obtained by Pspice simulation (Appendix 1). The models were built in Pspice and simulated to determine the first fifty harmonics. The simulated harmonic values were used as the default harmonic characteristics of corresponding nonlinear loads in the application. Apart from the harmonic data of the load, the application requires the per unit impedance data, the per unit base values and other information in Table 2.2 for determining the system voltages. After the data as described in Table 2.2 was obtained the values must be converted into per-unit values on consistent bases.

Per-unitizing the Data on Consistent Bases

The impedance data of the individual components supplied by the user are in per-unit format. The per-unit values are based on the corresponding kV and kVA values. The per-unit values should be based on consistent bases throughout the system. In order to be consistent, the supply voltage value entered by the user and a three-phase power base of 100 MVA are set internally as bases at the supply bus, Bus 1, of Figure 2.3. The supply source power base is used as to per-unitize the data on consistent bases. Initially, the SI values for individual components are found in order to convert to per-unit on consistent bases. Equations (2.3) and (2.4) are used to find the SI value of the supply source impedance. In (2.3), KV_s and KVA_s are the supply voltage in kV and the supply power in kVA respectively. The impedance base for the given per-unit values is calculated using (2.3). In (2.4), $\overline{Z}_{s,pu}$ is the given per-unit impedance value.

$$Z_{base} = \frac{KV_s^{\,2} * 1000}{KVA_s} \quad \Omega \tag{2.3}$$

$$\overline{Z}_s = Z_{base} * \overline{Z}_{s,pu} \quad \Omega \tag{2.4}$$

The capacitor and the load impedances are not directly given in per-unit. The transformer impedance value is given as per-unit magnitude, but the complex impedance is required for calculations. The capacitor, transformer and load impedance values (both resistance and reactance) are calculated from given power and voltage values.

The capacitor impedance is calculated using (2.5), where $KVAR_c$ and KV_c are the given kVAr and kV values of the capacitor. The impedance calculated in (2.5) is in SI units. The resistance of the capacitor bank is neglected.

$$-jX_c = -j\left(\frac{KV_c^2 * 1000}{KVAR_c}\right) \Omega \tag{2.5}$$

The impedance of the transformer is given as a percent and an X to R ratio. Z_{SI}, the transformer impedance value in SI units, is found using (2.6). In (2.6), KV_x is the phase-to-phase kV value of the transformer, KVA_x is the three-phase kVA value of transformer and %Z is the percent impedance of the transformer.

$$Z_{SI} = \left(\frac{\%Z}{100}\right) * \frac{KV_x^2 * 1000}{KVA_x} \quad \Omega \tag{2.6}$$

The Z_{SI} in (2.6) is the magnitude of the transformer impedance. The Z_{SI} value and the X to R ratio are used to find the complex transformer impedance value as in (2.7). Equation (2.7) results in a quadratic equation with R as the variable. X is found by multiplying the R with the X to R ratio. If the X to R ratio is entered as zero, then the resistance of the transformer is assumed to be zero and the reactance is set equal to the Z_{SI} value.

$$\left.\begin{aligned} Z &= \sqrt{R^2 + X^2} \\ &= \sqrt{R^2 + \left(\left(\frac{X}{R}\right) * R\right)^2} \end{aligned}\right\} \tag{2.7}$$

The nonlinear load is represented as an impedance at fundamental frequency. Equations (2.8) and (2.9) are used to find the nonlinear load impedance magnitude and the complex impedance, respectively, where θ_{pf} is the displacement power factor (DPF) angle of the load. In (2.10) θ_{pf} is calculated from the DPF value of the load. If the load DPF is lagging then θ_{pf} is positive; if the DPF is leading then θ_{pf} is negative.

$$Z_{load} = \frac{KV_{load}^2 * 1000}{KVA_{load}} \ \Omega \tag{2.8}$$

$$\overline{Z}_{load} = \left(Z_{load} * \cos(\theta_{pf})\right) + j\left(Z_{load} * \sin(\theta_{pf})\right) \ \Omega \tag{2.9}$$

$$\theta_{pf} = \pm\cos^{-1}(DPF) \tag{2.10}$$

Once the SI values are found, base values of voltage, power and impedance are calculated at every bus with respect to a reference bus. In this application, Bus 1 of Figure 2.3 is set internally as the reference bus. The phase-to-neutral voltage of the supply source, $\overline{V}_s$, calculated in (2.11) is set internally as the reference bus voltage. In (2.11) $V_{s,old}$ is the given supply source voltage.

$$\overline{V}_s = \left(\frac{V_{s,old}}{\sqrt{3}}\right)\angle 0° \tag{2.11}$$

The magnitude V_s in (2.11) is the voltage base at Bus 1. As mentioned before, in this application a three-phase power base of 100 MVA is assumed. Because the voltage base calculated in (2.11) is a line-to-neutral value, a single-phase power base should be used. The power base S_{base} (which is a single-phase quantity) is calculated as in (2.12). Once the voltage and the power bases are found, the impedance base is calculated using (2.13) where V_s is in kV and S_{base} is in MVA. The base values calculated at bus 1 remain the same for buses 2 and 3 assuming a lossless per-unit system. When crossing the transformer between buses 3 and 4, the voltage base value changes according to the transformer turns ratio. The voltage base value at bus 4 is calculated using (2.14) where V_{LV} and V_{HV} are the low voltage and the high voltage ratings of the transformer. The impedance base at bus 4 is calculated using (2.13) by replacing V_s with phase-to-neutral voltage $V_{base,4}$. The $V_{base,4}$ value in (2.14) is in kV. Because the harmonic current injection values are to be represented as sources for frequencies other than the fundamental, the current base at bus 4 is calculated using (2.15). After finding the base values at every bus the corresponding SI quantities of all the elements in the system in Figure 2.3 are per-unitized using these consistent bases.

$$S_{base} = \frac{100}{3} \text{ (MVA)} \tag{2.12}$$

$$Z_{base} = \frac{V_s^2}{S_{base}} \tag{2.13}$$

$$V_{base,4} = \frac{V_{LV}}{V_{HV}} * V_s \tag{2.14}$$

$$I_{base} = \frac{S_{base} * 1000}{V_{base,4}} \tag{2.15}$$

The SI values and the base values of voltage, power and impedance calculated previously are used in (2.16) to calculate corresponding per-unit values on consistent bases. In Equation (2.16) a_{pu} is a per-unit value, base is a base value and a_{SI} is an SI value. Once consistent per-unit values are calculated, the system admittance matrix and current injection vectors of the system in Figure 2.3 are formed.

$$a_{pu} = \frac{a_{SI}}{base} \tag{2.16}$$

Building the admittance matrix [Y] of the Network

An admittance matrix can be used to represent mathematically any power system network. The user supplies the component's positive and zero sequence impedances as input. In this work, the positive and the negative sequence impedances are assumed to be equal for all the components. For the capacitors and the transformer, however, all three-sequence impedances are assumed to be equal with the exception of connection type as appropriate. The following assumptions are made for modeling the system:

1. The system is positive phase sequence and is a balanced three-phase system at a fundamental frequency of 60 hertz.

2. The harmonic sources are represented as current sources at frequencies greater than the fundamental frequency (60 hertz).
3. The transformer core losses are not considered.
4. The skin effect at higher frequencies is neglected.

Positive phase sequence for system voltages and currents is generally assumed as a rule-of-thumb for power system analysis. In a balanced three-phase system, the triplen harmonic currents behave like zero sequence currents [2]. The harmonics of order 4,7,10 etc and 2, 5, 8 etc behave as positive sequence and negative sequence, respectively. When the phases are not balanced, any harmonic may impact all three sequences.

The distorted harmonic current can be expressed mathematically as the sum of sinusoidal waves at the individual frequencies present. The sum of these sinusoidal waves is called a Fourier series. Solving a system for bus voltages is easier when a Fourier series is used to represent distorted current waveforms [2]. By representing the harmonic sources as Fourier series, sinusoidal steady-state techniques can be used to solve the network. Conventional methods like the Kirchhoff's Current (KCL) and Kirchhoff's Voltage (KVL) Laws can be used. Therefore, the harmonic sources are modeled as current sources at individual harmonic frequencies.

The resistance of lines or cables does not change significantly for lower order harmonics. The skin effect of the conductors becomes significant at higher frequency where the resistance varies as the square root of the frequency [2]. For large transformers, the apparent resistance may vary proportionately with the frequency [2]. In any case, the variation of resistance with frequency cannot be accurately calculated. Besides, neglecting the frequency dependence of the resistance gives conservative results. Therefore, the frequency dependence of resistance is neglected.

Based on the assumptions stated previously, the admittance matrix is built internally by the application using the information provided by the user. The admittance matrix of an N bus power system network is in (2.17). In (2.17) $\overline{y}_{i,j}$ is the negative of the sum of all admittances connected between buses i and j and $\overline{y}_{i,i}$ is the sum of all admittances connected to bus i.

$$[\overline{Y}] = \begin{bmatrix} \overline{y}_{11} & . & . & \overline{y}_{1i} & . & \overline{y}_{1j} & . & . & \overline{y}_{1N} \\ . & . & . & . & . & . & . & . & . \\ . & . & . & . & . & . & . & . & . \\ \overline{y}_{i1} & . & . & \overline{y}_{ii} & . & \overline{y}_{ij} & . & . & \overline{y}_{iN} \\ . & . & . & . & . & . & . & . & . \\ \overline{y}_{j1} & . & . & \overline{y}_{ji} & . & \overline{y}_{jj} & . & . & \overline{y}_{jN} \\ . & . & . & . & . & . & . & . & . \\ . & . & . & . & . & . & . & . & . \\ \overline{y}_{N1} & . & . & \overline{y}_{Ni} & . & \overline{y}_{Nj} & . & . & \overline{y}_{NN} \end{bmatrix} \tag{2.17}$$

Every element in the admittance matrix is frequency dependent. In effect, every element is scaled depending on the harmonic number [2, 5]. Inductive reactances increase linearly with frequency and are scaled by multiplying them with h, the harmonic number (that is a multiple of 60 hertz). For example, if X_L is defined as the inductive reactance at the fundamental frequency of 60 hertz, then at a (h*60) hertz frequency it is equal to (h*X_L). Capacitive reactances reduce as the frequency increases. Capacitive reatances are divided by the harmonic number. For example, if X_C is defined as the capacitive reactance at the fundamental frequency of 60 hertz, then at a (h*60) hertz frequency it is equal to (X_C/h). As previously discussed, resistance is assumed to be constant with respect to frequency.

Depending on the harmonic number and the characteristic behavior of the corresponding frequency (such as positive, negative or zero sequence), different admittance matrices are formed. The negative and the positive sequence admittance matrices will be different because a different harmonic number is used to scale the admittances. After scaling the component admittances appropriately, they are added as $\overline{y}_{i,j}$ and $\overline{y}_{i,i}$ in (2.17) to form the system admittance matrix. The transformer admittance, however, should be added with caution.

Different types of transformer connections have different effects on system admittance matrices. Therefore, the modeling of transformers is different for different connections. The positive and the negative sequence impedances of the transformer are added to $\overline{y}_{i,j}$ and $\overline{y}_{i,i}$ in (2.17) using the procedure described previously for (2.17). Only the zero sequence admittance matrix is affected by the type of transformer connection. The pi circuit in Figure 2.4 is used to model the transformer for different types of connections. In Figure 2.4 $\overline{A}$, $\overline{B}$ and $\overline{C}$ are admittances defined in (2.18). In (2.18), c is the tap on the transformer and $\overline{Z}$ is the transformer impedance. The value of tap is calculated using (2.19) where $HV_{base\ (L\text{-}N)}$ is the transformer high voltage side phase-to-neutral voltage base value in kV and t is the phase-to-phase voltage supplied for tap in kV.

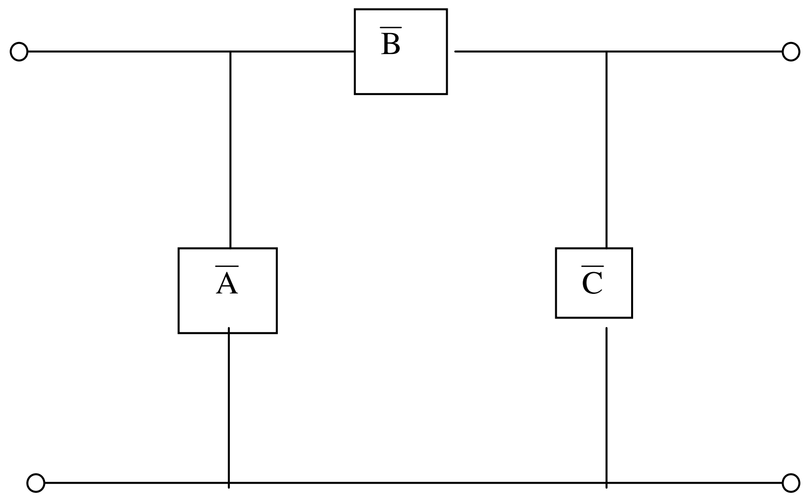

Figure 2.4. Pi Network

$$\left.\begin{aligned}\overline{A} &= (1-c)\left(\tfrac{1}{\overline{Z}}\right)\\ \overline{B} &= c\left(\tfrac{1}{\overline{Z}}\right)\\ \overline{C} &= (c^2-c)\left(\tfrac{1}{\overline{Z}}\right)\end{aligned}\right\} \tag{2.18}$$

$$c = \frac{t}{\sqrt{3} * HV_{base(L-N)}} \tag{2.19}$$

Figure 2.5 is the zero sequence network model of a transformer. Depending on the type of transformer connection, the ground impedances are added between nodes 1' and 1" and 2' and 2" in Figure 2.5 to complete the zero sequence network.

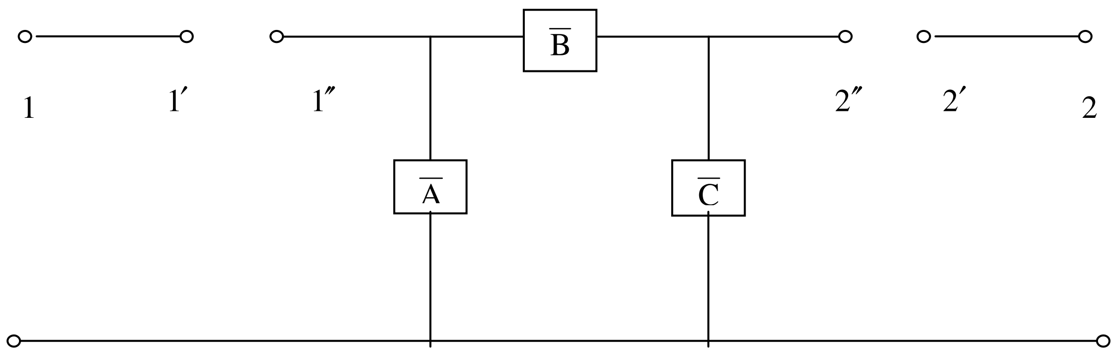

Figure 2.5. Zero Sequence Transformer Equivalent Network.

Consider node 1 of the circuit in Figure 2.5. If the transformer is connected in Δ at 1, then the path between nodes 1' to 1" is an open circuit and 1" is shorted to reference. The shorting of the node 1" to the reference due to a Δ connection is discussed in a later paragraph that explains the handling of a unity tap transformer. If the transformer is $Y_{grounded}$ at node 1, then nodes 1' to 1" are connected by an impedance equal to three times the grounding impedance. If the transformer is Y connected (ungrounded) at node 1, then path between nodes 1' to 1" is an open circuit. The procedure for including the connection type for node 1 is also used for node 2. A reactance of 10000 p.u is used internally to represent the infinite impedance of the open circuit for Δ and Y connections. The following steps summarize the procedure for including the transformer in the system zero sequence admittance matrix for a non-unity tap c:

1. The pi network admittances $\overline{A}, \overline{B}$ and $\overline{C}$ are inverted to get corresponding impedances defined as $\overline{a}, \overline{b}$ and $\overline{c}$. Note if the tap value is equal to 1 then the inversion of $\overline{A}$ and

$\overline{C}$ results in infinite values. The transformer connections for unity tap are discussed as a special case in a later paragraph.

2. Using (2.20), (2.21) and (2.22) the pi network is converted to the T network in Figure 2.6.

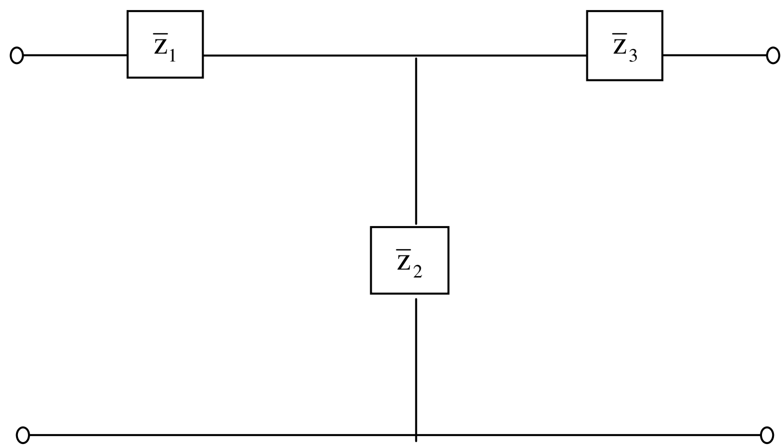

Figure 2.6. T Network Equivalent Representation of Transformer.

$$\overline{z}_1 = \frac{\overline{a} + \overline{b}}{\overline{a} + \overline{b} + \overline{c}} \tag{2.20}$$

$$\overline{z}_2 = \frac{\overline{a} + \overline{c}}{\overline{a} + \overline{b} + \overline{c}} \tag{2.21}$$

$$\overline{z}_3 = \frac{\overline{c} + \overline{b}}{\overline{a} + \overline{b} + \overline{c}} \tag{2.22}$$

3. The $3^*\overline{Z}_{grounding}$ or the j10000 p.u is added to the corresponding impedances ($\overline{z}_1$ and/or $\overline{z}_3$).

4. The T impedance values ($\bar{z}_1, \bar{z}_2, \bar{z}_3$) are converted back to the pi impedances ($\bar{a}, \bar{b}, \bar{c}$) using (2.23), (2.24) and (2.25).

$$\bar{a} = \frac{\bar{z}_1 * \bar{z}_2 + \bar{z}_2 * \bar{z}_3 + \bar{z}_1 * \bar{z}_3}{\bar{z}_1} \tag{2.23}$$

$$\bar{b} = \frac{\bar{z}_1 * \bar{z}_2 + \bar{z}_2 * \bar{z}_3 + \bar{z}_1 * \bar{z}_3}{\bar{z}_2} \tag{2.24}$$

$$\bar{c} = \frac{\bar{z}_1 * \bar{z}_2 + \bar{z}_2 * \bar{z}_3 + \bar{z}_1 * \bar{z}_3}{\bar{z}_3} \tag{2.25}$$

After converting the impedances back to admittances, the transformer admittance model is complete and the admittances $\bar{A}, \bar{B}$ and $\bar{C}$ are added to $\bar{y}_{i,j}$ and $\bar{y}_{i,i}$ in (2.17) using the procedure described previously for (2.17).

Consider a special case of a unity tap transformer. Let the transformer be a $Y_{grounded}$-Δ connected. Figure 2.7 represents the zero sequence network of a unity tap $Y_{grounded}$-Δ transformer. The zero sequence currents flow only in the $Y_{grounded}$ side of the network. The shorting of node 2″ makes a closed loop for the zero sequence currents to flow in the $Y_{gournded}$ side of the transformer. Admittances $\bar{A}$ and $\bar{C}$ are zero, i.e. the impedances corresponding to $\bar{A}$ and $\bar{C}$ are infinite. The ground impedance $3*\bar{Z}_{grounding}$ effects only node 1 in Figure 2.7. Admittance $\bar{y}$ in (2.26) is added to $Y_{from.from}$ of the network zero sequence admittance matrix. For $Y_{from,to}$, $Y_{to,from}$ and $Y_{to,to}$, there is no addition needed because the admittance is zero.

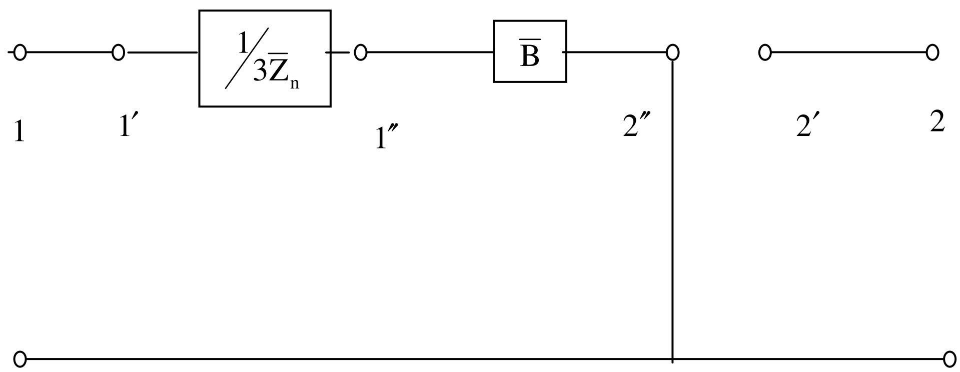

Figure 2.7. Zero Sequence Network for a Unity Tap $Y_{grounded}$-Δ Transformer.

$$\bar{y} = \frac{1}{3 * \bar{Z}_n} + \bar{B} \tag{2.26}$$

For a Δ-$Y_{grounded}$ unity tap transformer, an admittance equal to $\bar{y}$ in (2.26) is added to $Y_{to,to}$ entry of system admittance matrix and the $Y_{from,to}$, $Y_{to,from}$ and $Y_{to,to}$ are all added zero values. For a $Y_{grounded}$- $Y_{grounded}$ transformer, the procedure described for (2.17) is used to add the transfomer and the grounding admittances (based on three times the grounding impedance). For Δ-Δ, Δ-Y, Y-Δ and Y-Y connections the paths between nodes 1' to 1" and 2' to 2" are open circuit. Therefore, a zero admittance is added to the system admittance matrix using the procedure described for (2.17).

At this point, the mathematical modeling of the system considered for this study is complete. The next step is to form the current injection matrix and solve for bus voltages.

System Response

The harmonic currents injected by nonlinear loads are required to find the harmonic bus voltages in the system. Eight commonly used nonlinear loads are provided for default use. The nonlinear loads considered in this study are:

1. Single-phase power supply,
2. Semi-converter,
3. Six pulse converter with capacitive smoothing,
4. Six pulse converter with capacitive smoothing 3% series inductance (or DC drive),
5. Six pulse converter with large inductor for current smoothing,
6. Twelve pulse converter,
7. AC voltage regulator, and
8. Fluorescent lighting.

For most of the loads, the harmonic current data provided was obtained from the simulated values of case studies from the Superharm manual [4, 6]. However, a few were simulated using Pspice (Appendix 1). In general, harmonics from 1 to 50 are studied in most harmonic analyses and typical monitoring equipment measures the same range. Therefore, only the first 50 harmonics are considered in this work. If measured harmonic data is available and is different from the typical data provided, the user can modify the data and the modified data is used to find the system response. In the absence of measured data, the typical values available in the application can be used for studying the harmonic impact on the system.

Once the frequencies present for a particular nonlinear load are known, their behavior is then categorized as positive sequence (h = 1, 4, 7…), negative sequence (h = 2, 5, 8…) and zero sequence (h = 3, 6, 9…). For individual frequencies present, the current injection vector $\tilde{\bar{I}}$ of the network is formed. The size of the current injection vector $\tilde{\bar{I}}$ is equal to the number of buses in the system. At any frequency the current injection vector $\tilde{\bar{I}}$ has only one nonzero value. At the fundamental frequency only the supply source is the power input to the network (recall that the load is represented as an impedance at the fundamental frequency). The user gives the voltage equivalent of the supply source as an input to the application. Therefore, the Norton equivalent circuit in Figure 2.8 can be used to represent the supply source at the fundamental frequency. The Norton equivalent circuit converts a voltage source to an equivalent current source. At frequencies higher than the fundamental, the supply source has only an impedance effect on the system.

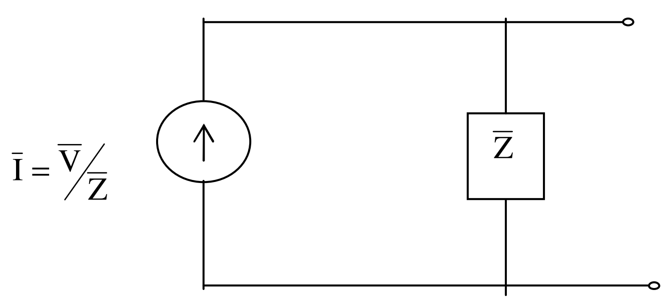

Figure 2.8. Norton Equivalent Circuit.

For frequencies higher than the fundamental, the nonlinear loads act as the input to the network. For frequencies other than the fundamental, the nonzero entry in the current injection vector $\tilde{\bar{I}}$ corresponds to the load bus. For the system in Figure 2.3, the (4, 1) entry in the current injection vector $\tilde{\bar{I}}$ would be nonzero and the remaining entries would be zero.

The nonzero values used in the current injection vector $\tilde{\bar{I}}$ should be in per-unit because the impedance values are in per-unit. The harmonic current data is supplied as a percent of the fundamental frequency load current magnitude and the angles are in degrees with respect to the bus voltage to which the load was connected. These percent current magnitudes need to be converted to SI values and then per-unitized on a consistent base before using them to solve for bus voltages. The bus 4 fundamental frequency voltage value and the load impedance value are used to convert the percent values of the harmonic current magnitudes to per-unit values on a consistent base.

The fundamental frequency bus 4 voltage value is found by solving the network for bus voltages at the fundamental frequency. The network model at the fundamental frequency consists of the Norton equivalent of the supply source and the impedances of all the other components. Because the fundamental frequency behaves as positive sequence, the transformer connections do not effect the network connections. Using the techniques discussed earlier, the admittance matrix $[\bar{Y}]_1$ and the current injection vector $\tilde{\bar{I}}_1$ are formed where the subscript indicates the harmonic number being studied. The network is solved for fundamental frequency bus voltages using (2.27). In (2.27) $\tilde{\bar{V}}_1$ and

$\tilde{\bar{I}}_1$ are the per-unit voltage and current vectors at the fundamental frequency. The admittance matrix $[\bar{Y}]_1$ used in (2.27) is a positive sequence admittance matrix.

$$\tilde{\bar{V}}_1 = [\bar{Y}]_1^{-1} * \tilde{\bar{I}}_1 \quad (2.27)$$

Phase-to-neutral voltage and single-phase power values are used as bases, therefore, (2.27) gives the per unit values of the phase-to-neutral bus voltages. Once the per-unit value of the bus 4 fundamental voltage is found, the fundamental load current is then found using (2.28). In (2.28) $\bar{Z}_{load}$ is the per-unit load impedance and $\bar{V}_{4,1}$ is the bus 4 voltage at fundamental frequency in per-unit.

$$\bar{I}_{4,fundamental} = \frac{\bar{V}_{4,1}}{\bar{Z}_{load}} \quad (2.28)$$

In (2.28) $\bar{I}_{4,fundamental}$ represents the per-unit value of the fundamental frequency load current. Equation (2.29) is used to scale the percent harmonic current magnitudes and (2.30) is used to scale the angles with respect to the supply source phase-to-neutral voltage. In (2.29) $I_{h,percent}$ and $I_{1,percent}$ are the (order h) harmonic current and fundamental current magnitudes in percent and $I_{h,new}$ is the scaled per-unit value of (order h) harmonic current injection. In (2.30) $\theta_{h,old}$ and $\theta_{h,new}$ are the old and the modified current angles of the order h harmonic, $\theta_{4,fundamnetal}$ is the $\bar{I}_{4,fundamental}$ angle at the fundamental frequency and $\theta_{1,old}$ is the old fundamental current angle.

$$I_{h,new} = I_{h,percent} * \frac{1}{I_{1,percent}} * I_{4,fundamental} \quad (2.29)$$

$$\theta_{h,new} = \theta_{h,old} + h * (\theta_{1,old} - \theta_{4,fundamental}) \quad (2.30)$$

In (2.30) the subscript "old" represents the value given as input data. Using the current vector and the system admittance matrix in per-unit formed on a consistent bases, the system bus voltages can then be found.

The bus voltages are found for each harmonic by solving (2.31). In (2.31) $\tilde{\bar{V}}_h$ is the per-unit voltage vector and $\tilde{\bar{I}}_h$ is the per-unit current injection vector for harmonic h. The bus impedance matrix $[\bar{Z}]_h$ is the inverse of the bus admittance matrix $[\bar{Y}]_h$. The Shipley-Coleman method of matrix inversion is used for the admittance matrix inversion because of its simplicity [3]. The values used in (2.31) and the results of solving (2.31) are in per-unit. These per-unit values are converted to SI values using the same bases used for converting them to per-unit.

$$\tilde{\bar{V}}_h = [\bar{Z}]_h * \tilde{\bar{I}}_h \tag{2.31}$$

The voltages found from (2.31) are line-neutral voltages. The phase angles of the voltages of buses with the transformer connected to them may need to be adjusted with the appropriate phase shift of ±30º [7]. If the transformer is delta-wye connected, then the load bus voltage angle for any harmonic order h that is a positive sequence is shifted by (-h*30) degrees. For harmonics that are negative sequence, the shift is (+h*30) degrees. The triplen harmonics (those that are an integer multiple of the 3^{rd} harmonic) are not affected by the phase shift.

The procedure described up to this point is used to find the system response for multiple nonlinear loads. Therefore, the final results of computing the bus voltages would be the single-phase line-to-neutral voltages with appropriate phase shift added to the angles. Figure 2.9 is the flow chart of the entire logic behind calculating the system response.

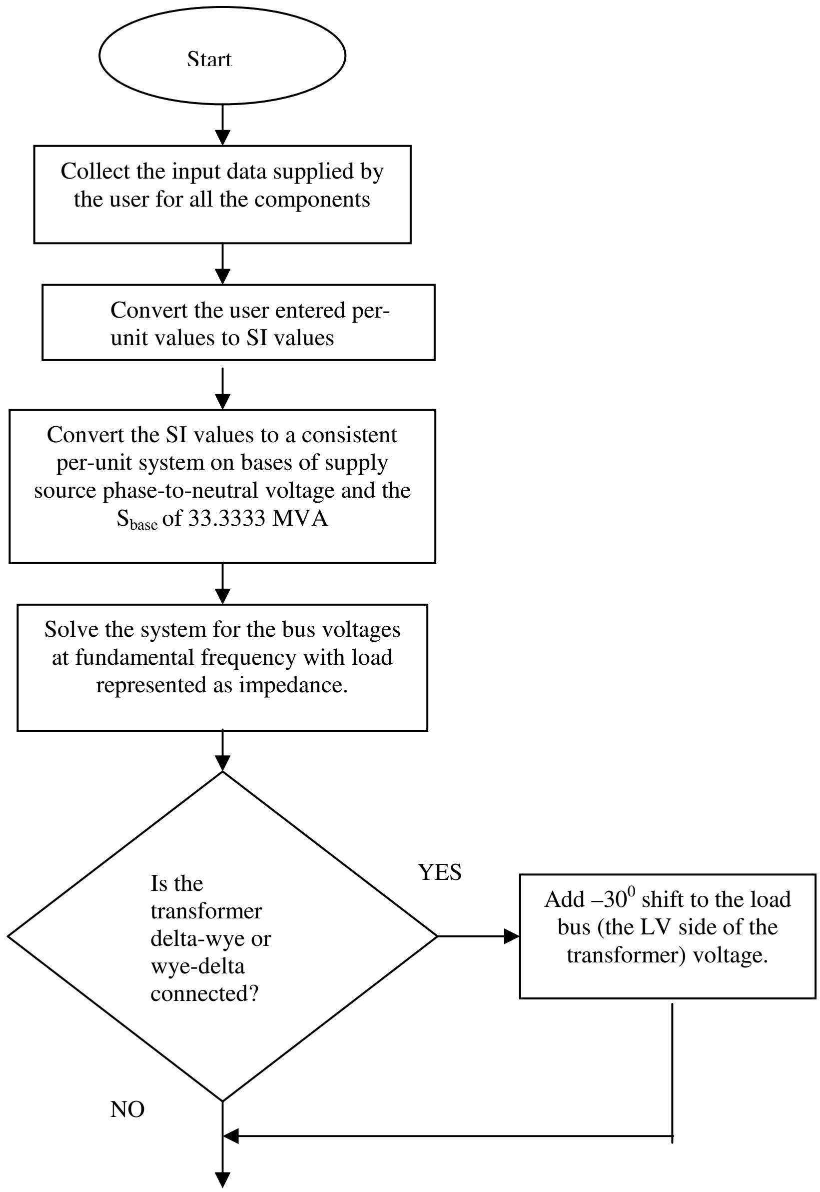

Figure 2.9. Flowchart with the Logic Used in Finding the System Response.

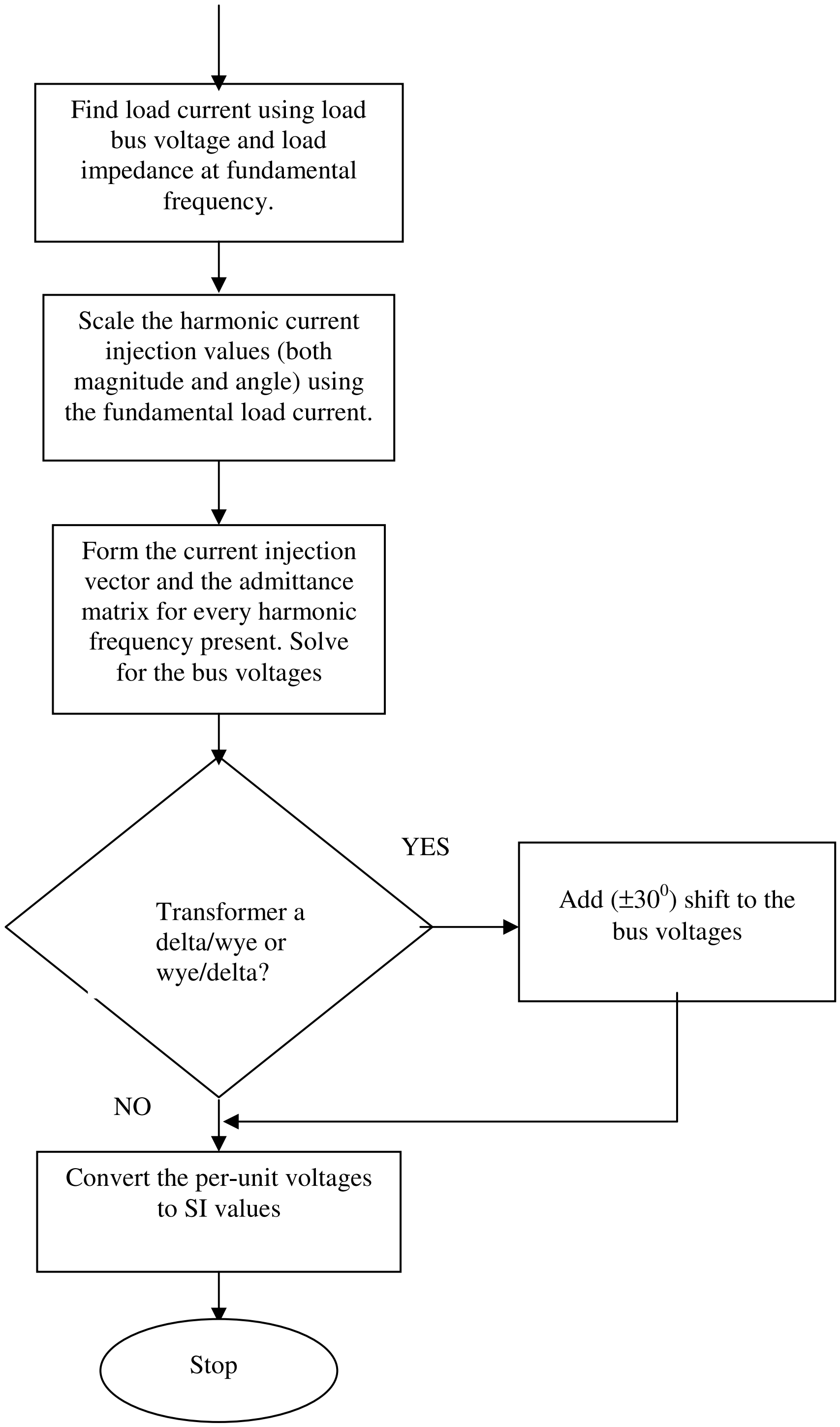

Figure 2.10. Figure 2.9. (continued)

CHAPTER III

THE GUI FEATURES

Introduction

In the previous chapter discussion of the logical part of the application was given. In this chapter the description of the graphical user interface (GUI) part of the work is given. The software application developed is a Microsoft Windows-based application. The Microsoft foundation classes (MFC) of the Visual C++ programming language were used to develop the GUI features of this application. A proper design using the MFC tools like Cdialog box, Cview and Cdocument classes [8] will result in a user-friendly and easy to use application. The user interface can be designed in several ways by using the properties and functions associated with the Cdialog, Cview and other classes of the MFC.

MFC applications are mainly of two types - a single document interface or a multiple document interface [8]. In a single document interface only one client space or main window is used to display results, waveforms etc. Figure 3.1 is a sample single document interface application.

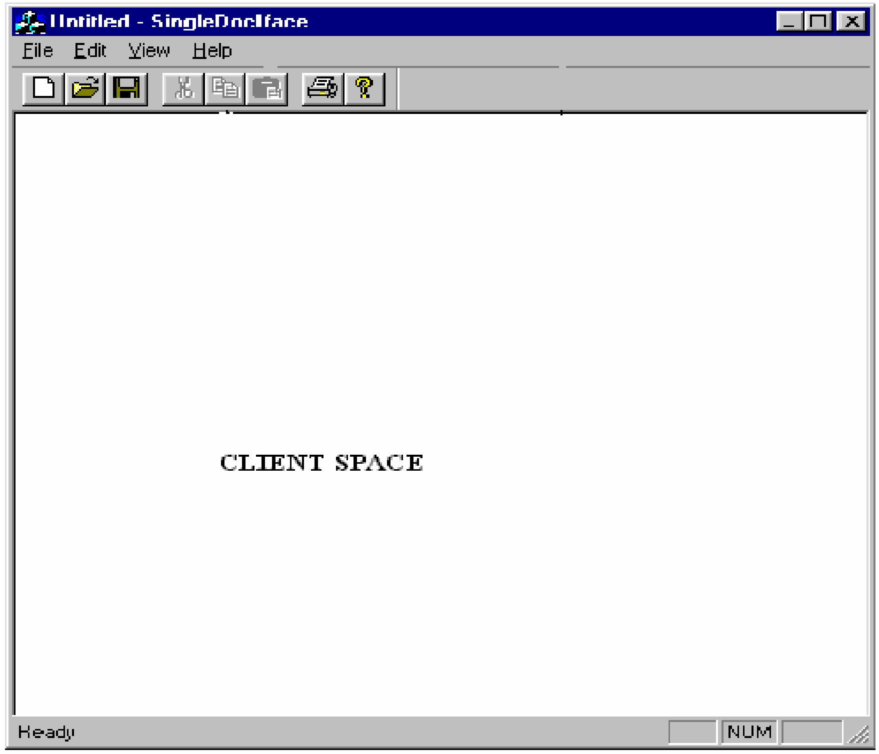

Figure 3.1. Sample Application of Single Document Interface.

The “client space” area in Figure 3.1 can be used as a workspace. The developer (or the programmer) may use the client space to display some data or to draw diagrams. In this thesis the client space is used to display the waveforms, bar diagrams and a grid to present data.

A developer could develop a multi-document interface (MDI) application. A sample MDI is in Figure 3.2. In a multiple document interface there are many windows or “client spaces” known as child windows. All child windows are associated with one mainframe window. Different child windows can be opened or closed depending on the type of application developed, but by closing the mainframe window all the child windows close. Apart from the child windows in Figure 3.2, dialog boxes can also be used in an MDI application. The application developed in this thesis work is MDI and uses different dialog boxes as child windows.

Figure 3.2. A Sample MDI Application Frame.

Dialog boxes belong to the Cdialog class of the MFC. Dialog boxes make windows-based programs user interactive. There are two types of dialog boxes: modal and modeless. A modal dialog box does not allow the user to work on another window in the same application as long as the dialog box is open. The modeless dialog box, however, gives the user the flexibility to access another window with the modeless dialog box still open on the screen. This property of a modeless dialog box allows the user to swap between child windows. Both modal and modeless dialog boxes are used in this thesis work.

The modal and modeless dialog boxes used in this thesis work are designed using various controls associated with them. The user supplies data to the application through dialog box controls. Figure 3.3 is a sample dialog box showing some of the dialog box controls used in this application. The different controls used in Figure 3.3 are briefly described in the following paragraphs.

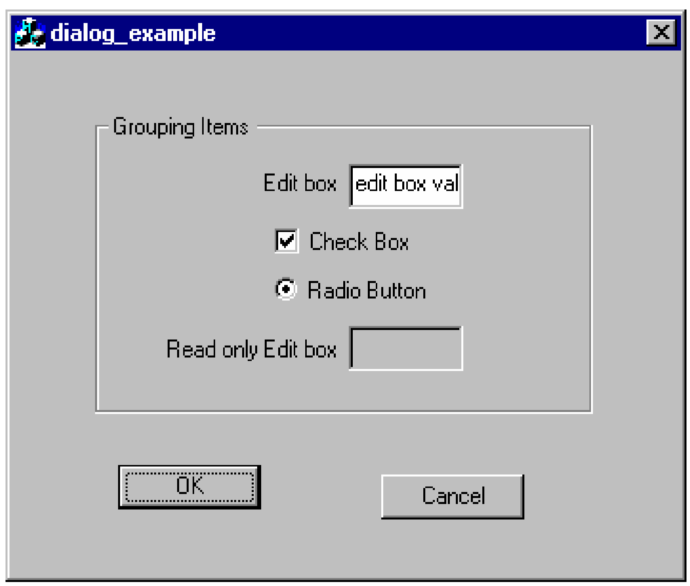

Figure 3.3. Sample Dialog Box with Most Common Controls.

The control labeled "Edit box" in Figure 3.3 is a static control. Static controls are used to display names for controls. The rectangular box with "edit box val" is an edit control. The user types input data into an edit control and then this input data is passed to the application. For example, the kVA value of the load is entered in an edit box labeled (using a static control) “kVA value.” Another edit control used is a read-only edit box. A read-only edit box displays alpha-numerical content which cannot be edited or accessed by the user.

Radio buttons and check boxes are two other controls. The “value” of these two controls can be toggled between true or false by a single mouse click. For example, the displacement factor of the load can be specified as lagging by clicking on a radio button labeled as “lag.” In Figure 3.3 the small circle and the small rectangular box are a radio button and a check box, respectively.

Another control in Figure 3.3 is the grouping static control labeled “Grouping items.” This control is used for designing the display of a dialog box. The grouping control is used for giving a set of controls that are related to one another as a single name. It is also used for seperating different groups of controls that perform different functions on a single dialog box.

The data entered in a dialog box is processed when the user clicks a control called a Cbutton control. These controls are used to send messages to the main application program. For example an “OK” button is clicked to pass the data entered to the main program. In the application described here, bitmaps are placed over the cbuttons to give an enhanced look to the dialog box.

The cgridctrl developed by Chris Maunder [9] was used for designing some of the dialog boxes in the application. A typical cgridctrl is in Figure 3.4. The cgridctrl properties like the size (number of colums and rows), the nomenclature and the scrolling bars of the grid were changed to fit the application in this thesis.

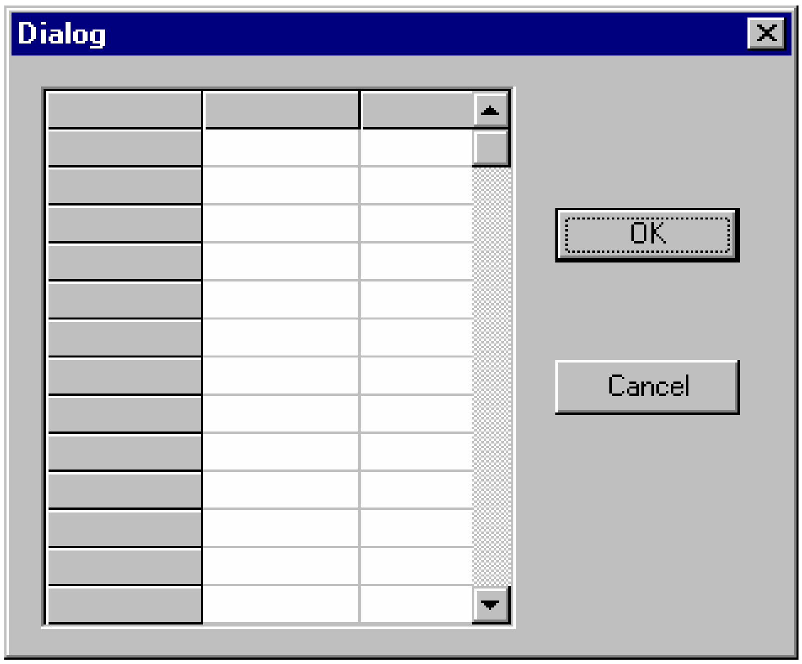

Figure 3.4. Sample Dialog Box with Grid.

The controls described in the previous paragraphs were used to design the dialog boxes used in the application described in this thesis. A sample dialog box with most of these controls is in Figure 3.5.

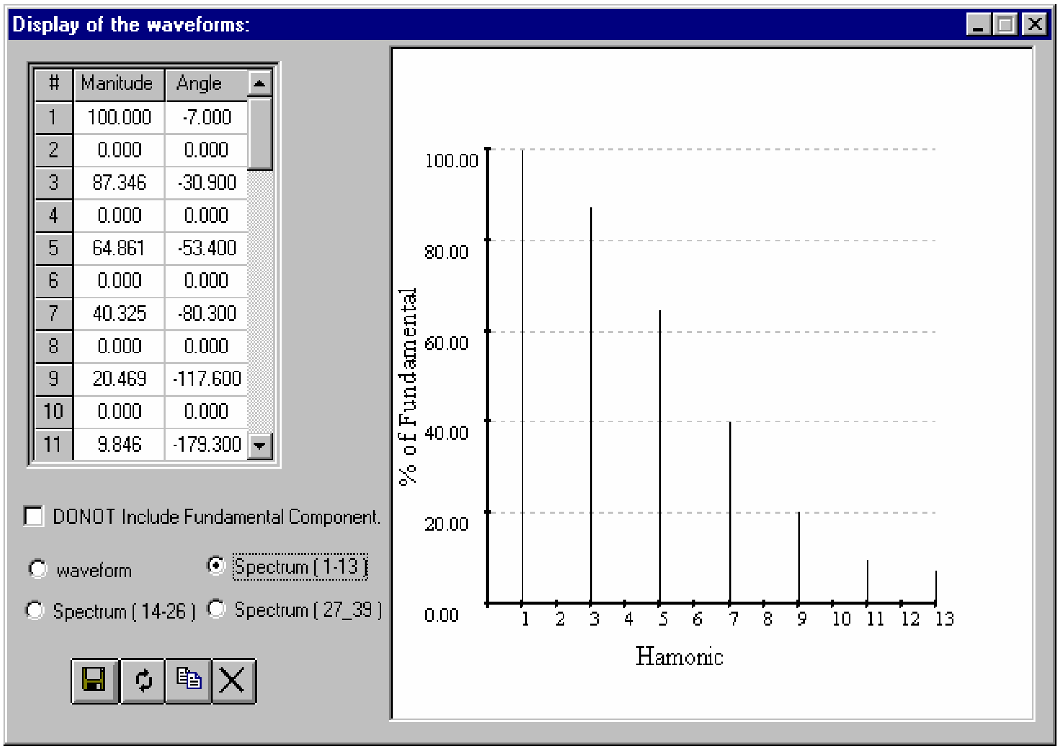

Figure 3.5. Sample Dialog box with Grid Used in the Application.

In the bottom-left of the dialog box in Figure 3.5 there are buttons for different purposes. If the user changes the values in the grid then the modified display can be viewed by pressing the refresh button in Figure 3.6. Apart from refreshing the display the user can also save the changes in the harmonic data points in the grid by pressing the button in Figure 3.7. The modified values in the grid data are stored internally in the application and are used for any further calculations.

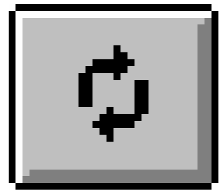

Figure 3.6. Button for Refreshing the Display.

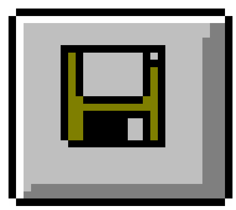

Figure 3.7. Button for Saving the Modified Data Values of the Grid.

The user also has the choice of copy-pasting just the display (waveform/spectrum) into a Microsoft Word document for recording or report writing purposes by clicking the button in Figure 3.8. When the user clicks this button the plot is copied into clipboard. The user can then paste the picture in a Word document. One last button in the dialog box is the close button in Figure 3.9 and is used to close the dialog box as. After the design aspect of the application is completed, dialog boxes and other child windows are systematically integrated in to the mainframe window of the application.

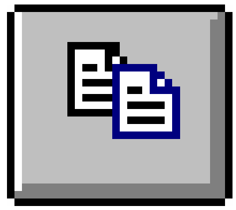

Figure 3.8. Button for Copying the Plot.

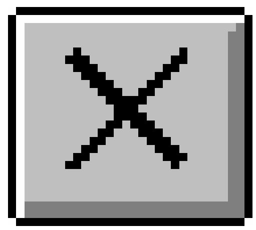

Figure 3.9. Button for Closing Dialog Box.

Different Tasks in the Development of the Final Application

From displaying the study system considered in this thesis work to displaying the resulting distorted waveforms, all the tasks are developed in a step-by-step procedure. The tasks assigned for the GUI code can be summarized as the following:

1. Displaying the system diagram and retrieving the data from the user.
2. Applying the automatic acceptance criteria (AAC) to the given data.
3. Generating and displaying the plot (waveform/spectrum) for the data entered.
4. Verifying the required data and display any error message.
5. Passing the data to the code for the solution.
6. Displaying bus harmonic voltages (magnitudes and angles) and the waveforms.

Displaying the System Network

The single line diagram representation of the system is displayed in a child window as in Figure 3.10. In Figure 3.10 the supply system is represented as a circle and the capacitor banks by short horizontal parallel lines. The vertical parallel “jaws” represent the transformer. The nonlinear load is represented as a square box. The thick vertical bars represent the buses in the network. Two cable lines are considered in the system, one from the supply bus to the first capacitor bank and the other is the line between the first capacitor and the transformer. A single mouse click on an individual component of the system displays the dialog box describing that component.

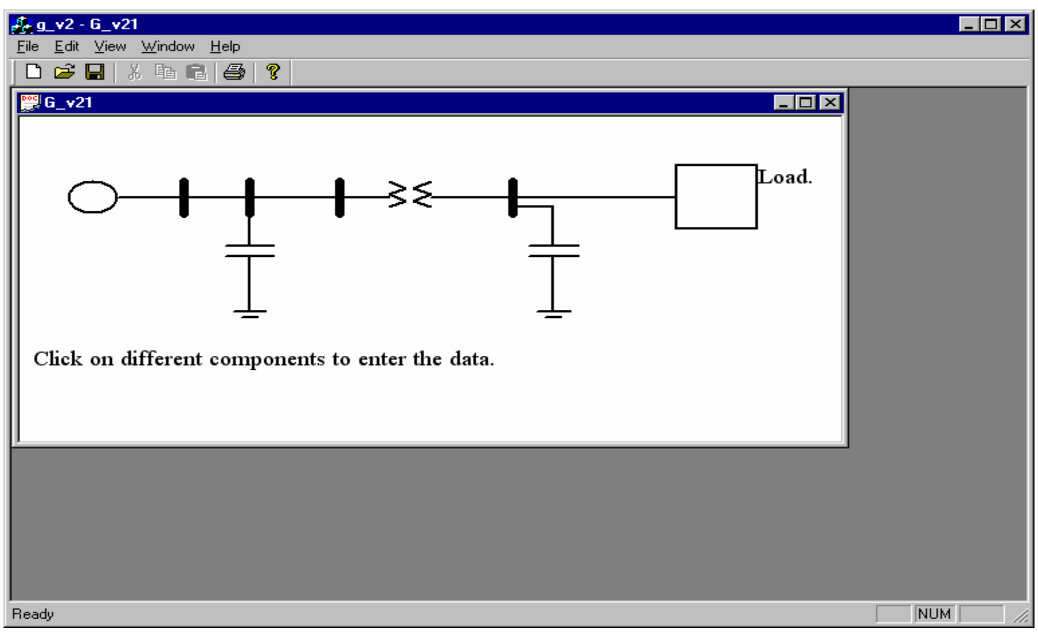

Figure 3.10. Display of the Network Considered for the Study.

Collecting the Data for Different Components

The dialog box in Figure 3.11 is for entering the data for the supply source. The per-unit values of the positive and zero sequence impedance of the supply source are to be entered in the edit boxes specified. The kVA and the kV values are three-phase and phase-to-phase quantities, respectively. A default value of 100,000 kVA is internally set in the application. However, the user can change the kVA value.

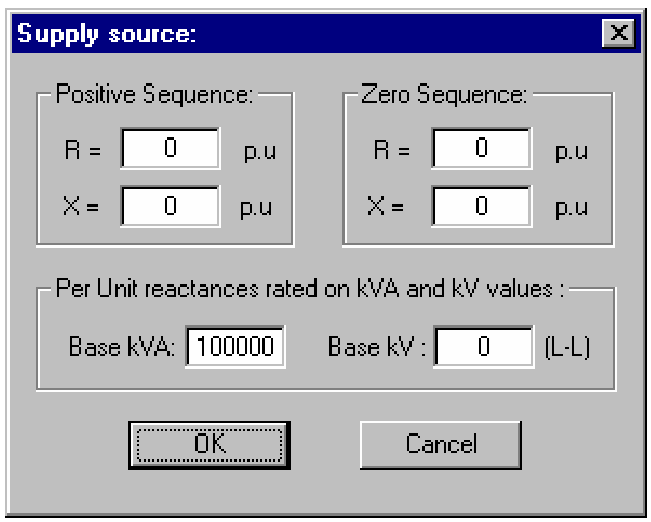

Figure 3.11. Dialog Box for the Supply Source.

The dialog box for the lines and cables is in Figure 3.12. The per-unit values supplied by the user should be based on the kV and the kVA values entered. A default value of 100,000 kVA is internally set for the line kVA value. However, the user can modify the kVA value. The voltage entered in the dialog box should be a phase-to-phase kV value.

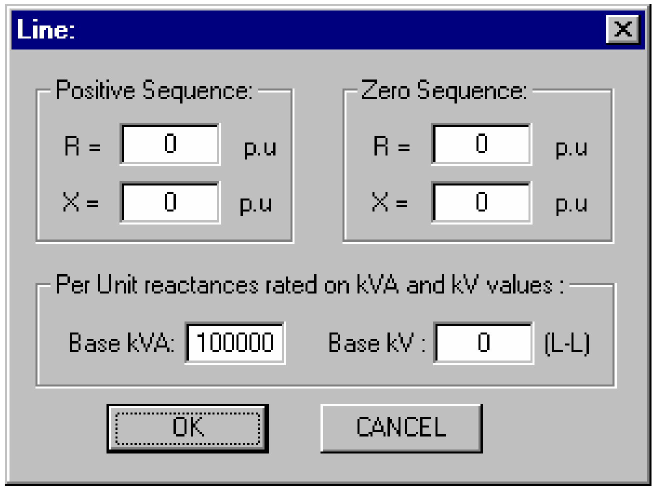

Figure 3.12. Dialog Box for the Line data.

The dialog box in Figure 3.13 is used for the capacitors. The three-phase kvar and the kV(L-L) values of the capacitor are supplied through this dialog box.

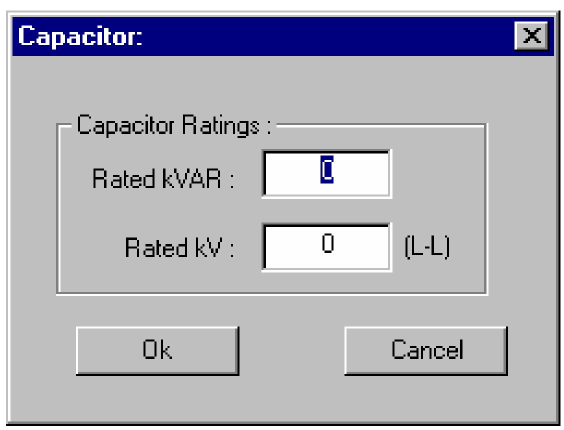

Figure 3.13. Dialog Box for the Shunt Capacitor Ratings Data.

The dialog box in Figure 3.14 is used for entering the transformer details. The transformer turns ratio is entered as the high voltage and the low voltage values in phase-to-phase kV. The kVA rating should be a three-phase quantity. The grounding impedances (if any) are to be entered in ohms. The tap of the transformer is set on the high voltage side and is to be entered in terms of phase-to-phase volts in kV. Because the transformer considered is a three-phase transformer, the user needs to specify the type of connection on both the high voltage and the low voltage side of the transformer by clicking on the radio buttons.

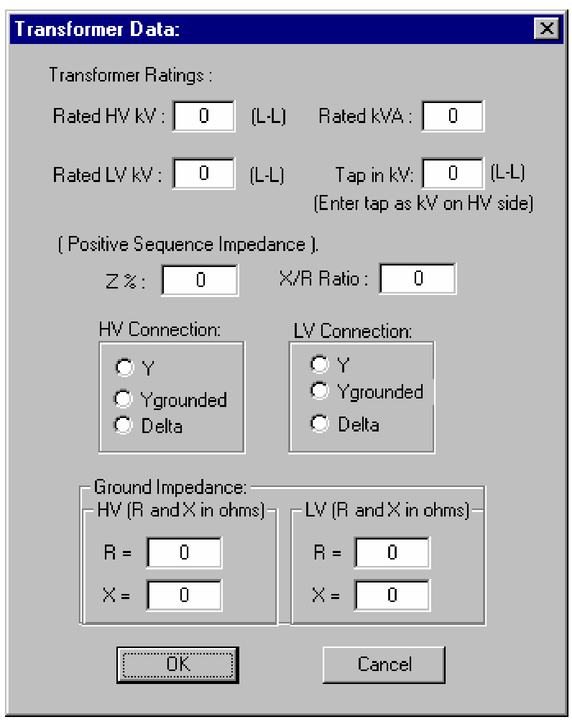

Figure 3.14. Dialog Box for Entering the Transformer Data.

Nonlinear Loads

When the user clicks on the load represented by the rectangular box the dialog box in Figure 3.15 pops up. The user can enter the phase-to-phase kV and the three-phase kVA values of the loads. The main purpose of the dialog box in Figure 3.15 is to apply the AAC and estimate if the entered quantities of nonlinear loads could cause any potential harmonic problems. The user can enter the short circuit capacity at the PCC and then click on the “COMPUTE” button. The application then computes the weighted distorting power from the given set of data and displays it in the edit box named “Weighted Distorting Power (in kVA) is found to be.” The ratio of weighted distorting power to the short circuit power and the limit of 0.1% (set in AAC approach for potential harmonic problems) are displayed. This part of the application gives the user a quick estimate of any potential harmonic problem. Clicking any of the “PLOT” buttons in the dialog box, in Figure 3.15, pops up a dialog box with the typical waveform/spectrum of the corresponding nonlinear load.

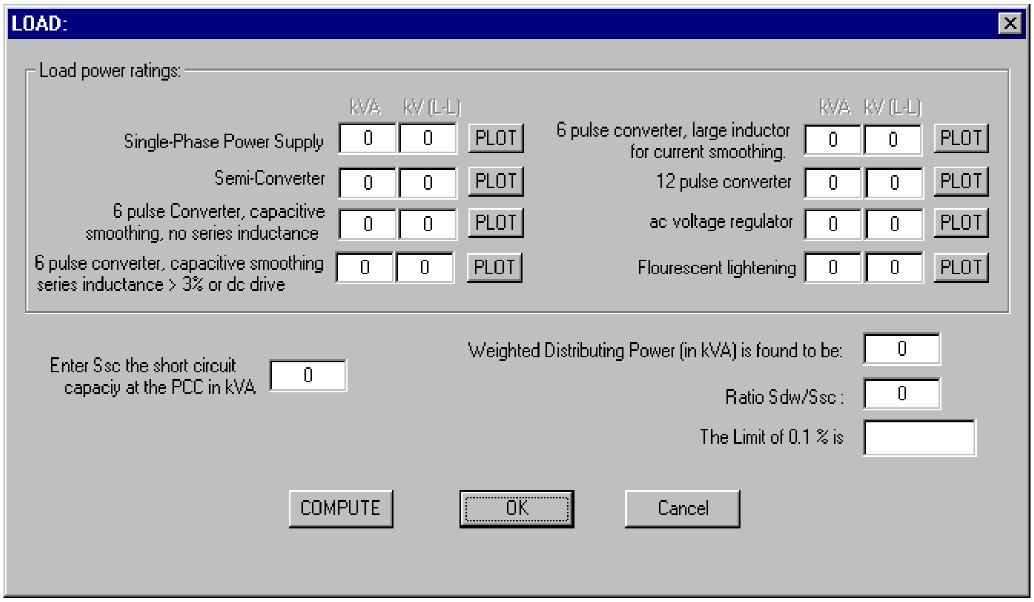

Figure 3.15. Dialog Box for kVA and kV Load Values.

Developing the Plot for the Nonlinear Load

Apart from applying the AAC, the user can view the harmonic current data corresponding to individual non-linear loads and the associated waveform/spectrum by clicking the "PLOT" button. When the user clicks the "PLOT" button a dialog box as in Figure 3.16 pops up. This gives the user the choice of calling the axes of the waveform plot by any name. When the user clicks the "OK" button these names are passed to the plotting function and the dialog box in Figure 3.17 pops up.

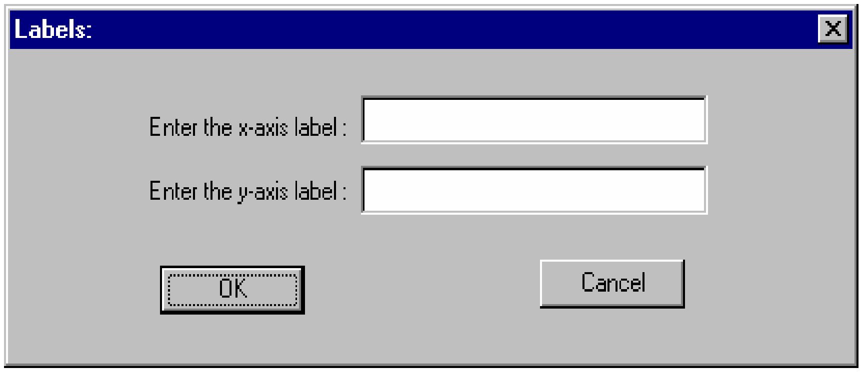

Figure 3.16. Dialog Box for the x and the y-axes Labels.

The dialog box in Figure 3.17 contains the grid control that is used to display the typical harmonic current data for the selected nonlinear load. The harmonic number, the corresponding magnitude (in percent of the fundamental current) and the angle (in degrees) are displayed in this grid. The grid is used to display both the current and the voltage harmonic data. In the case where current harmonic data are displayed (for the nonlinear load), the user can modify the data (which is typical harmonic data as mentioned in Chapter 2) if actual measured data is available. Depending on the interest of the user, the user can also edit the voltage harmonic data.

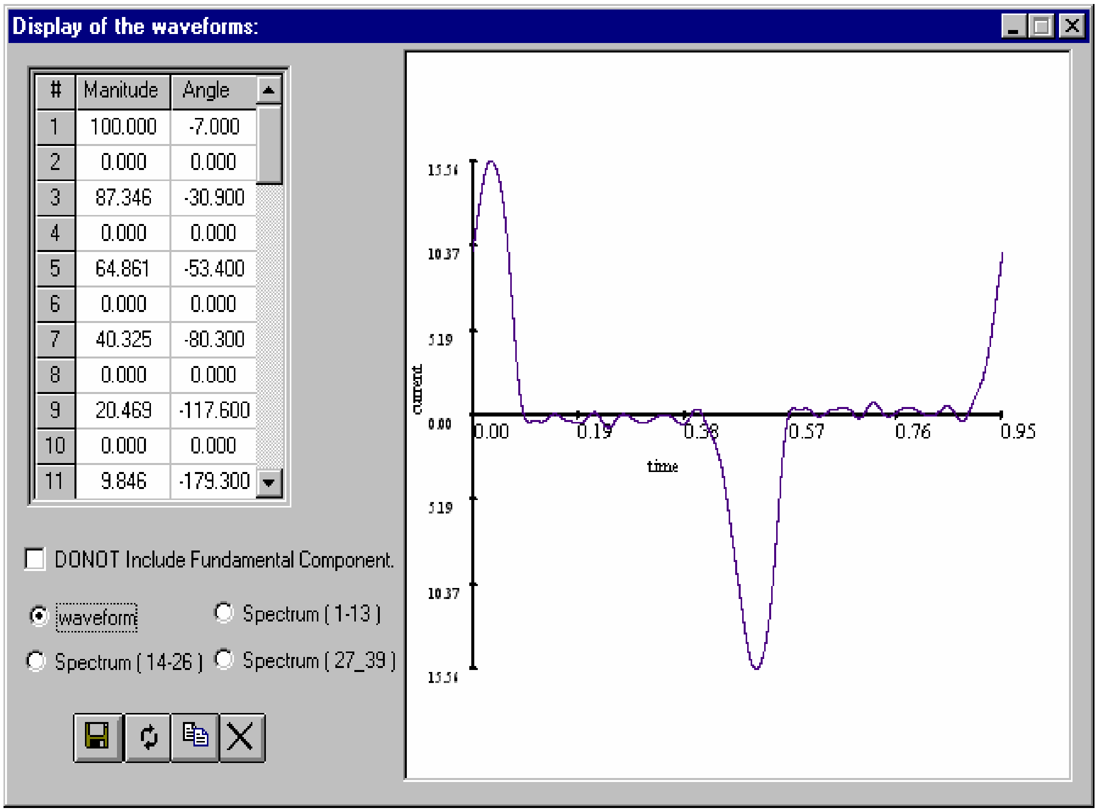

Figure 3.17. Dialog Box with the Harmonic Data and Waveform for Single-phase Power Supply.

The plot in the right hand side of the dialog box in Figure 3.17 is generated using the values in the grid. Clicking on the “Spectrum” radio button displays the spectrum on the right hand side of the dialog box. The “Spectrum” names also suggest the range of harmonic numbers for which the spectrum would be displayed like 1 to 13, etc. Because the viewing space is small, the spectrum is divided into three ranges to have a clear view of the individual harmonics. Figure 3.18 is a spectrum display for one of the nonlinear loads. When the user selects “DO NOT Include Fundamental” in the dialog box in Figure 3.18 and clicks on the refresh button, the bar plot of the first 13 harmonics are redrawn excluding the fundamental. This feature is included in the dialog box because most of the higher harmonics are small as compared to the fundamental. For example the fundamental would usually be 100% but maybe the 5th harmonic would be just 15%. Such a low percent value may appear artificially small on the plot and the user would be misled.

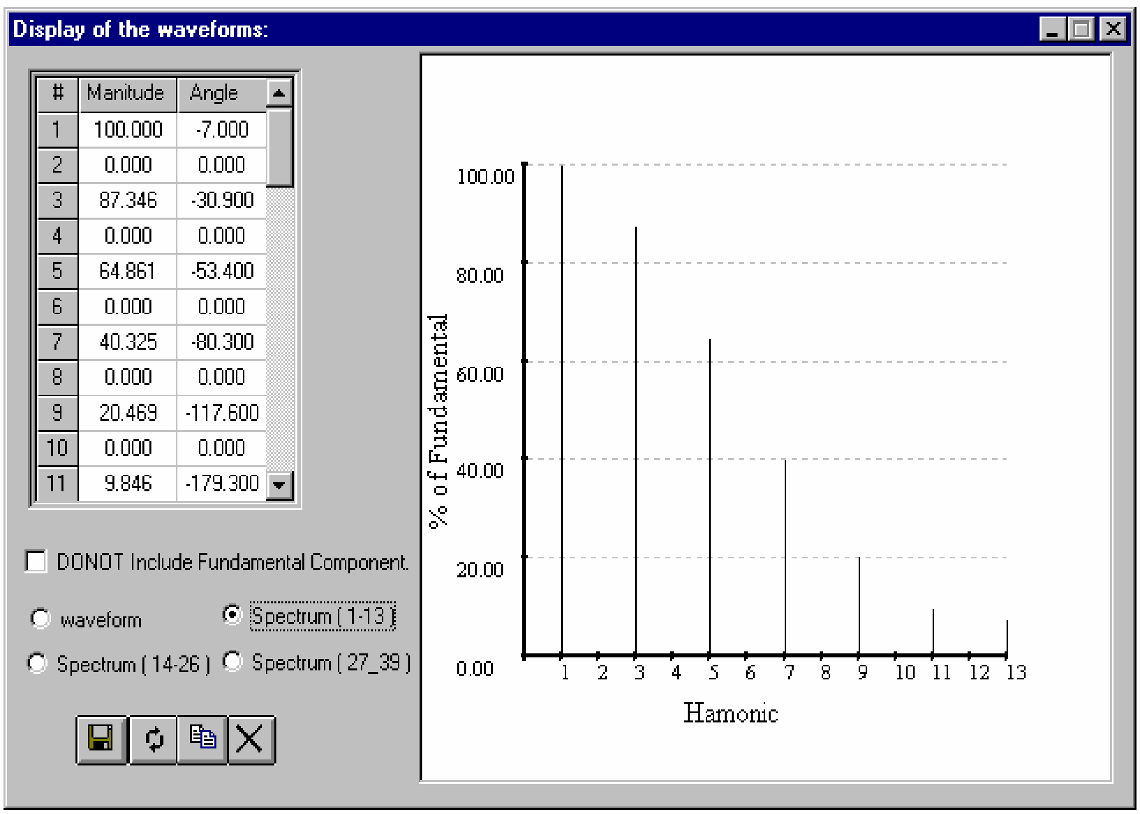

Figure 3.18. Dialog Box with the Harmonic Data and Spectrum for Single-phase Power Supply.

After the user finishes entering the harmonic current data and the kV and kVA values for the load, the dialog box in Figure 3.19 pops up. The dialog box in Figure 3.19 is used for entering the nonlinear load data.

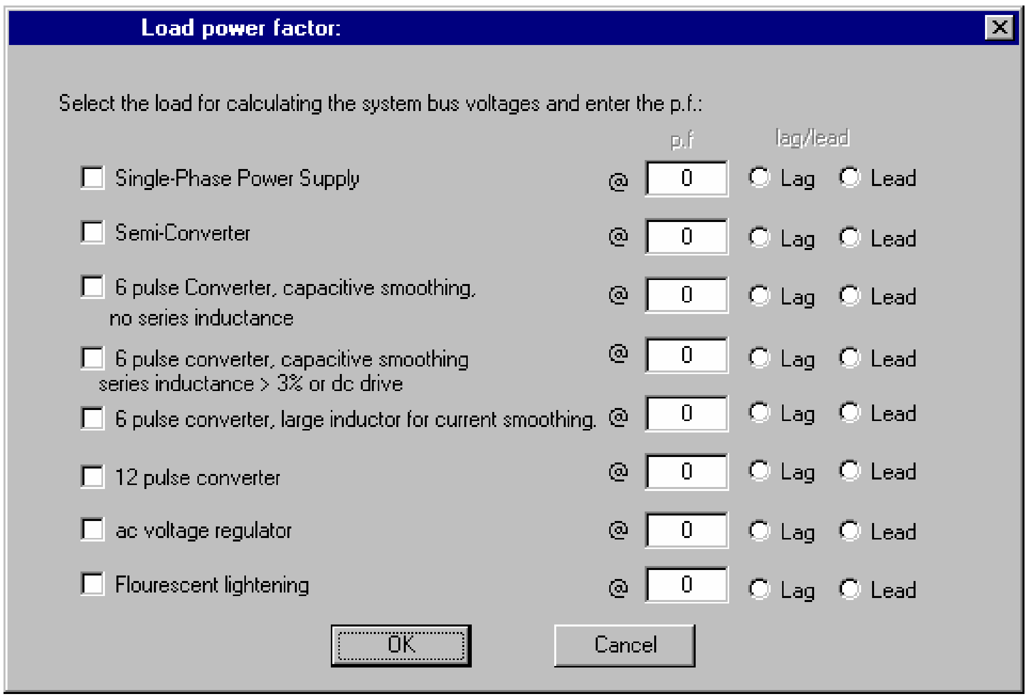

Figure 3.19. Dialog Box for Selecting Load and Corresponding Power Factor of Load.

The dialog box is used in selecting different kinds of nonlinear loads to be considered for the finding the bus voltages. The edit boxes and radio buttons in the dialog box of Figure 3.19 furnish the information regarding the load power factors. This information is required for doing any further analysis. Therefore, the dialog box in Figure 3.18 is a modal dialog box. The user can not access the rest of the application unless the dialog box is closed. Once the user enters the data for all the individual components of the system and the nonlinear load, the user can then click on any bus of interest to view the harmonic voltages.

Verifying the Data and Displaying Error Message

When the user clicks on the bus, the dialog box with the harmonic voltage magnitude and angle values and the corresponding plot (waveform/spectrum) is displayed. However, if the user fails to furnish all the information needed then the computed harmonic voltage values could be erroneous. Therefore, when the user clicks on any bus to examine the harmonic voltages, the application calls a validating function. This function verifies if all the information for every component in the system has been provided by the user and displays an error message if any is missing. The dialog box in Figure 3.20 with the error message pops up if any data is missing. The error message gives the user the a description of the information that is not supplied to the application.

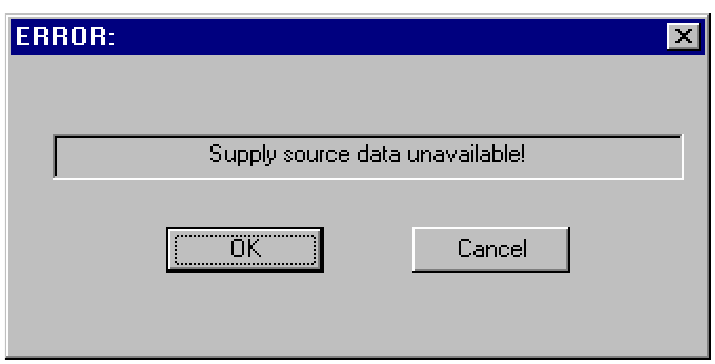

Figure 3.20. Dialog Box with the Error Message.

All the values typed in or selected by the user in the dialog boxes described up to this point are passed to the solution algorithm through the member functions and properties of MFC classes. Figure 3.21 is the flowchart that represents the sequence in which the user could use the application.

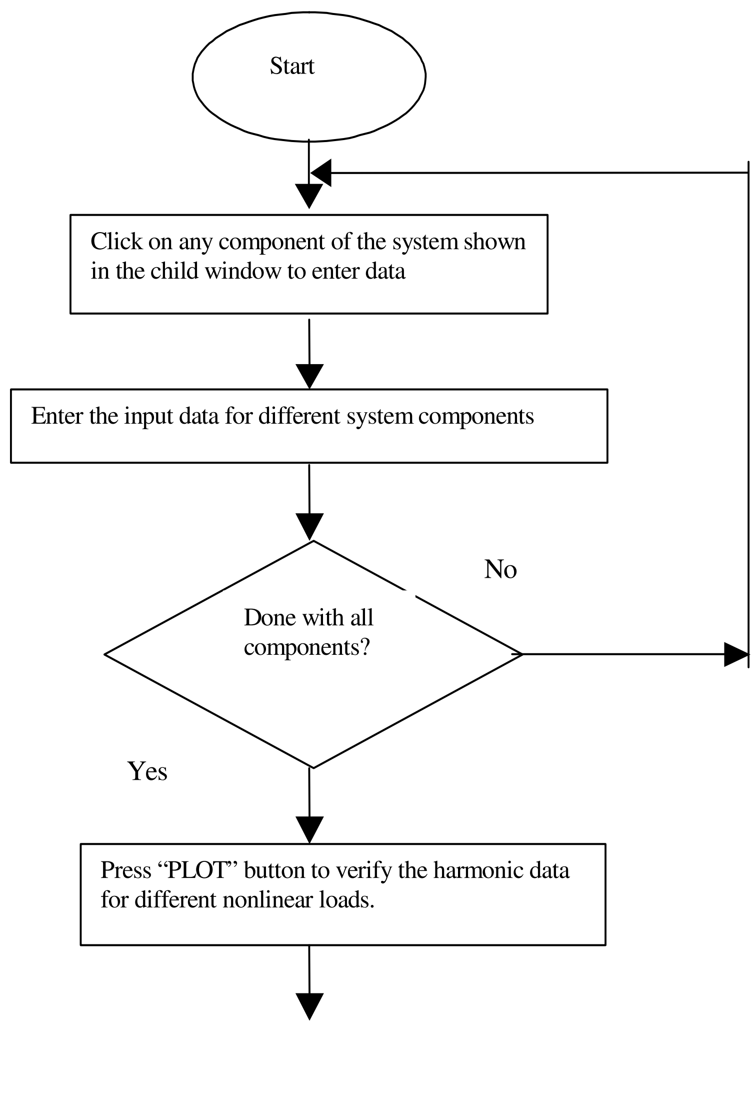

Figure 3.21. Flowchart with Typical User Interface Sequence.

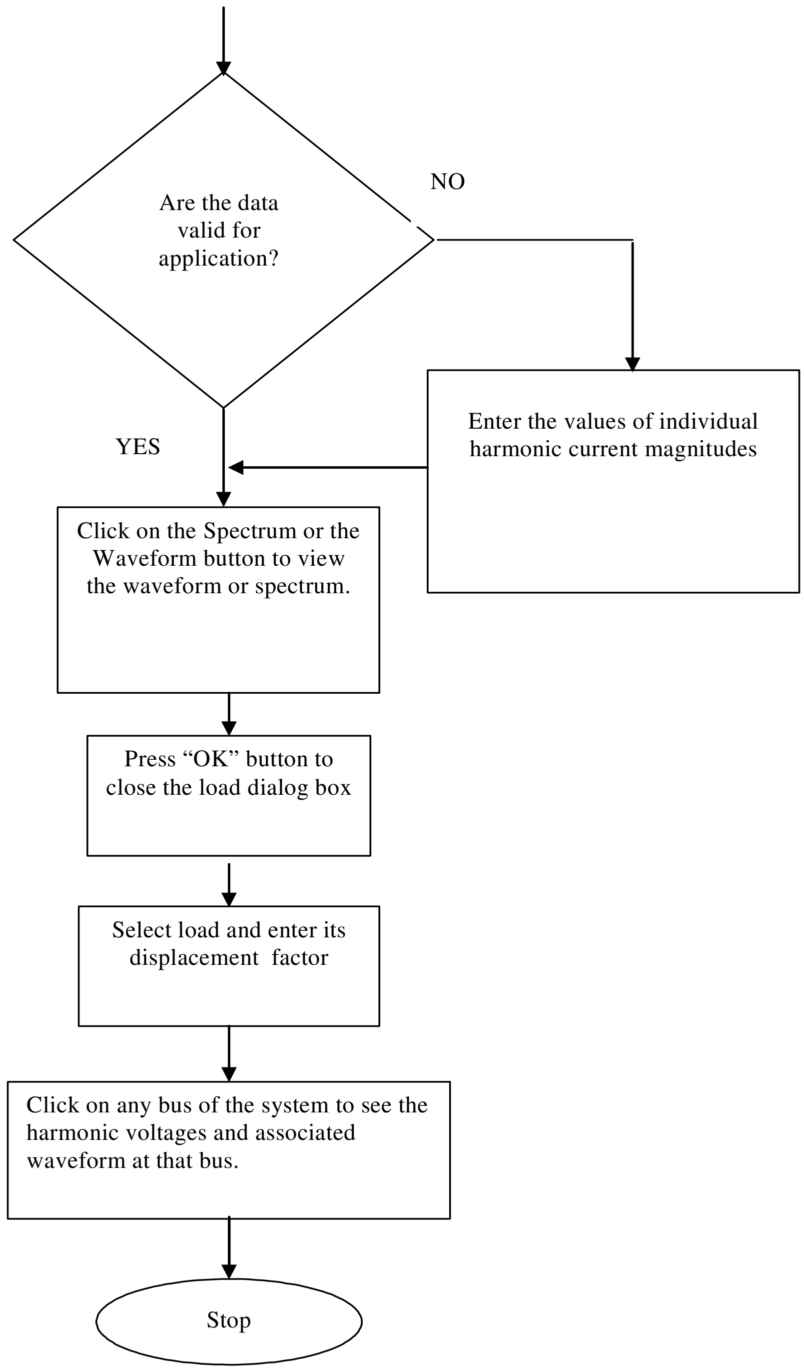

Figure 3.22. Figure 3.21 (continued)

CHAPTER IV

SAMPLE CASES AND RESULTS

To analyze the accuracy of the application, sample cases were run using the application and a commercial-grade application (Superharm). The sample cases are used to assess the accuracy of numerical and graphical data as compared to results obtained using Superharm.

Two sample cases were used to illustrate the accuracy of the application. Case 1 has two six pulse converters as the nonlinear loads, and the second case is continuation of the first case with the changes in the capacity of the nonlinear load.

Case 1:

The system data for the sample case is in Table 4.1

Table 4.1. Data for Sample Case 1.

Component name	**Data Supplied by the User**
Supply Source	1. Three phase kVA of 200,000 kVA 2. Phase to phase kV of 13.8 kV 3. Positive sequence of (0.05+j1.0) in per unit based on the given kVA and kV values 4. Zero sequence of (0.039498+j0.89498) in per unit based on given kVA and kV values

Table 4.1 (continued)

Component name	Data Supplied by the User
Cable or Line (Between bus 1 and bus 2)	1. Three phase kVA of 100,000 kVA 2. Phase to phase kV of 13.8 kV 3. Positive sequence of (0.78555+j4.205) in per unit based on given kVA and kV values 4. Zero sequence of (0.5562+j4.21655) in per unit based on the given kVA and kV values
Shunt Capacitor (At bus 2)	1. Three phase kVAr of 700 kVAr 2. Phase to phase kV of 13.8 kV
Cable or Line (Between bus 2 and bus 3)	1. Three phase kVA of 100,000 kVA 2. Phase to phase kV of 13.8 kV 3. Positive sequence of (0.66525+4.6251) in per unit based on given kVA and kV values 4. Zero sequence of (0.55287+j4.18804) in per unit based on the given kVA and kV values
Transformer	1. Three phase kVA of 1500 kVA 2. Phase to phase high voltage kV of 13.8 kV 3. Phase to phase low voltage kV of 0.48 kV 4. Percent impedance (%Z) of 4% 5. X to R ratio of 5 6. Tap in kV on the HV side of 13.8 kV. 7. △-Y transformer connection. 8. Grounding resistance and reactance on HV and LV sides of zero ohms.
Shunt Capacitor (At bus 4)	1. Three phase kVAr of 700 kVAr 2. Phase to phase kV of 0.48 kV
Load 1 (6 pulse converter with capacitive smoothing)	1. Three phase kVA 150 kVA 2. Phase to phase voltage kV of 0.48 kV 3. Power factor (displacement factor) of 0.75 lag 4. Harmonic (h=1 to 50) current magnitudes in percentage of the fundamental and angle in degrees in Table 3 of Appendix
Load 2 (6 pulse converter with capacitive smoothing and a series inductor of >3%)	1. Three phase kVA 150 kVA 2. Phase to phase voltage kV of 0.48 kV 3. Power factor (displacement factor) of 0.75 lag 4. Harmonic (h=1 to 50) current magnitudes in percentage of the fundamental and angle in degrees in Table 4 of Appendix.

Assume bus 4 is the PCC. The short circuit capacity is calculated to be 551 kVA. The weighting factor for 6 pulse converter with capacitive smoothing is 2.0 and for 6 pulse converter with capacitive smoothing and a series inductor of >3% is 1.0. Therefore, the weighted capacity of the two nonlinear loads is calculated in (4.1).

$$\left.\begin{aligned} S_{DW} &= 150.0 * 2.0 + 150.0 * 1.0 \\ &= 450.0 \text{ kVA} \end{aligned}\right\} \tag{4.1}$$

$$\frac{S_{DW}}{S_{SC}} = \frac{450.0}{551} * 100 = 81\% \tag{4.2}$$

From (4.2), it can be concluded that the AAC limit of 0.1% is exceeded. The voltage wave distortions can be anticipated to be high because of the very high deviation from the 0.1%. Because the limit of 0.1% of the ratio of weighted capacity and the short circuit capacity is exceeded, a comprehensive harmonic analysis should be performed.

The results from the application program are tabulated in Table 4.2. To verify the accuracy of the harmonic bus voltage magnitude and angles generated by the application, they are compared with the Superharm simulation results. Table 4.2 are the results from the application and Table 4.3 are the Superharm results. In Tables 4.2 and 4.3 the "Mag" represents the magnitudes in volts, the "Angles" represent angles in degrees and "H#" is harmonic number. There is an error of 10 volts at lower harmonics. This could be because of difference in modeling of the transformer between Superharm and the application developed. However, with the voltage range in discussion in this case (i.e. 13.8 kV), the difference of 10 V is negligible.

Table 4.2. Results of the Sample Case 1 Using the Application.

H	Bus 1		Bus 2		Bus 3		Bus 4	
#	Mag	Angle	Mag	Angle	Mag	Angle	Mag	Angle
1	7991.16	-0.12	8174.21	-1.30	8172.56	-2.26	281.38	-32.80
2	0.57	127.47	5.45	123.30	9.76	125.65	0.43	155.83
3	0.00	0.00	0.00	0.00	0.00	0.00	0.45	1.83
4	3.09	146.87	23.88	130.89	35.09	145.78	1.32	117.66
5	298.62	-124.46	2858.85	-128.12	2906.42	-121.04	126.07	-89.21
6	0.00	0.00	0.00	0.00	0.00	0.00	0.36	34.95
7	94.55	141.98	885.46	132.44	881.81	146.60	2.51	160.01
8	9.05	22.56	17.62	55.08	19.96	55.21	0.39	-103.53
9	0.00	0.00	0.00	0.00	0.00	0.00	2.78	134.94
10	0.40	-2.69	12.75	6.64	14.82	7.64	1.09	153.78
11	19.58	125.47	196.12	132.54	198.03	132.82	24.46	-19.76
12	0.00	0.00	0.00	0.00	0.00	0.00	3.10	-175.19
13	8.29	25.97	70.99	31.71	74.21	35.27	14.54	-178.38
14	0.02	-97.78	0.37	-92.27	1.29	-92.51	0.09	118.48
15	0.00	0.00	0.00	0.00	0.00	0.00	3.13	52.78
16	0.02	155.78	0.24	165.81	1.30	169.87	0.09	-46.72
17	0.79	-162.63	8.73	-141.85	10.15	-142.76	3.59	55.48
18	0.00	0.00	0.00	0.00	0.00	0.00	0.24	29.36
19	0.32	139.60	4.12	140.86	5.43	142.06	1.67	-71.10
20	0.01	75.51	0.20	79.51	1.80	80.01	0.11	-74.59
21	0.00	0.00	0.00	0.00	0.00	0.00	0.53	159.82
22	0.01	83.92	0.17	87.39	0.22	88.65	0.09	-125.02
23	0.03	127.70	0.42	122.91	1.05	122.14	0.31	-30.66
24	0.00	0.00	0.00	0.00	0.00	0.00	0.08	-167.23
25	0.02	64.55	0.30	70.22	0.50	70.12	0.30	-142.67
26	0.01	-110.18	0.08	-110.78	0.12	-110.25	0.08	102.17
27	0.00	0.00	0.00	0.00	0.00	0.00	0.15	7.36
28	0.00	-154.20	0.01	-160.65	0.02	-160.02	0.02	-9.73
29	0.01	-124.82	0.12	-121.24	0.24	-120.87	0.16	90.22
30	0.00	0.00	0.00	0.00	0.00	0.00	0.01	11.27
31	0.01	96.22	0.16	97.25	0.28	95.06	0.26	-117.62
32	0.00	112.96	0.02	117.72	0.01	116.43	0.02	-36.32
33	0.00	0.00	0.00	0.00	0.00	0.00	0.04	170.86
34	0.00	62.14	0.02	62.34	0.02	62.34	0.03	-150.04
35	0.00	-151.91	0.03	-155.06	0.03	-155.27	0.06	56.47
36	0.00	0.00	0.00	0.00	0.00	0.00	0.01	109.13

Table 4.2 (continued)

H #	Bus 1		Bus 2		Bus 3		Bus 4	
	Mag	Angle	Mag	Angle	Mag	Angle	Mag	Angle
37	0.00	-22.62	0.06	-25.67	0.10	-25.32	0.13	126.86
38	0.00	-95.85	0.01	-100.00	0.01	-98.65	0.02	112.18
39	0.00	0.00	0.00	0.00	0.00	0.00	0.03	-7.62
41	0.00	-174.44	0.02	-175.04	0.02	-175.41	0.05	36.13
42	0.00	0.00	0.00	0.00	0.00	0.00	0.01	-31.63
43	0.00	172.48	0.03	175.08	0.03	175.44	0.07	-37.73
44	0.00	107.11	0.01	107.01	0.00	109.02	0.01	-44.56
45	0.00	0.00	0.00	0.00	0.00	0.00	0.03	113.18
46	0.00	-35.90	0.00	-14.11	0.01	-11.78	0.01	138.53
47	0.00	57.71	0.01	57.47	0.01	56.05	0.03	-95.32
49	0.00	84.02	0.01	85.23	0.01	85.37	0.03	-127.91
50	0.00	-145.91	0.00	-145.06	0.01	-145.05	0.02	65.70

Table 4.3. Results of the Sample Case 1 Using the Superharm.

H #	Bus 1		Bus 2		Bus 3		Bus 4	
	Mag	Angle	Mag	Angle	Mag	Angle	Mag	Angle
1	7990.66	-0.12	8170.03	-1.30	8111.74	-2.25	280.94	-32.78
2	0.55	128.81	5.21	125.31	9.66	126.03	0.42	155.87
3	0.00	-88.15	0.00	-90.49	0.00	-89.70	0.45	1.89
4	2.31	148.36	21.72	146.61	31.81	147.62	1.31	117.82
5	303.25	-119.67	2855.08	-121.07	3351.26	-119.66	126.39	-89.08
6	0.00	129.51	0.00	128.34	0.00	130.63	0.36	35.06
7	93.51	143.86	880.16	142.86	350.48	148.14	2.50	160.10
8	1.66	53.02	15.66	52.14	1.53	-152.43	0.39	-103.38
9	0.00	-148.27	0.00	-149.05	0.00	26.92	2.77	135.11
10	1.32	6.58	12.43	5.88	15.60	-176.37	1.09	153.97
11	20.77	132.56	195.42	131.92	378.19	-49.67	24.44	-19.55
12	0.00	113.63	0.00	113.04	0.00	-68.20	3.08	-174.92
13	7.36	33.44	69.26	32.90	241.64	-148.13	14.52	-178.14
14	0.04	-89.85	0.34	-90.35	1.50	88.77	0.09	118.74
15	0.00	141.93	0.00	141.46	0.00	-39.31	3.50	52.01
16	0.03	164.75	0.24	164.31	1.48	-16.38	0.09	-46.42

Table 4.3 (continued)

H #	Bus 1		Bus 2		Bus 3		Bus 4	
	Mag	Angle	Mag	Angle	Mag	Angle	Mag	Angle
17	0.87	-140.52	8.15	-140.93	60.12	38.45	3.43	68.40
18	0.00	120.26	0.00	119.88	0.00	-60.70	0.24	29.70
19	0.32	140.20	3.05	139.84	29.56	-40.70	1.67	-70.74
20	0.02	76.67	0.18	76.32	2.02	-104.17	0.11	-74.22
21	0.00	-109.17	0.00	-109.50	0.00	70.04	0.53	160.21
22	0.01	86.18	0.12	85.87	1.68	-94.57	0.09	-124.61
23	0.04	120.53	0.37	120.22	5.61	-60.19	0.31	-30.23
24	0.00	-76.18	0.00	-76.48	0.00	103.14	0.08	-166.78
25	0.03	68.49	0.29	68.21	5.37	-112.16	0.30	-142.20
26	0.01	-106.69	0.07	-106.95	1.38	72.69	0.08	102.65
27	0.00	99.24	0.00	98.98	0.00	-81.36	0.15	8.69
28	0.00	-158.59	0.02	-158.84	0.39	20.84	0.02	-9.20
29	0.01	-118.65	0.12	-118.89	2.94	60.80	0.16	90.76
30	0.00	102.34	0.00	102.10	0.00	-78.19	0.01	11.83
31	0.02	93.50	0.16	93.28	4.63	-87.01	0.26	-117.04
32	0.00	114.80	0.01	114.58	0.35	-65.69	0.02	-35.73
33	0.00	-98.06	0.00	-98.27	0.00	81.47	0.04	171.48
34	0.00	61.09	0.01	60.89	0.50	-119.37	0.03	-149.40
35	0.00	-152.40	0.03	-152.60	1.00	27.16	0.06	57.12
36	0.00	-159.77	0.00	-159.96	0.00	19.80	0.01	109.80
37	0.01	-21.99	0.05	-22.18	2.27	157.58	0.13	127.55
38	0.00	-96.67	0.01	-96.85	0.42	82.92	0.02	112.89
39	0.00	83.52	0.00	83.34	0.00	-96.88	0.03	-6.89
41	0.00	-172.70	0.02	-172.87	0.97	6.92	0.05	36.89
42	0.00	59.54	0.00	59.37	0.00	-120.84	0.01	-30.84
43	0.00	173.46	0.02	173.30	1.34	-6.90	0.07	-36.93
44	0.00	106.64	0.00	106.48	0.23	-73.71	0.01	-43.74
45	0.00	-155.62	0.00	-155.78	0.00	24.03	0.03	114.02
46	0.00	-10.25	0.00	-10.40	0.12	169.41	0.01	139.39
47	0.00	55.92	0.01	55.77	0.51	-124.41	0.03	-94.44
49	0.00	83.34	0.01	83.20	0.60	-96.98	0.03	-127.00
50	0.00	-143.03	0.00	-143.17	0.32	36.66	0.02	66.64

When the user clicks on any bus, the dialog boxes with the harmonic voltage at that bus pops up. Figures 4.1, 4.2, 4.3 and 4.4 are the dialog boxes with the harmonic voltage data and associated waveforms for buses 1, 2, 3 and 4 respectively. As stated earlier, the voltage wave has high distortions.

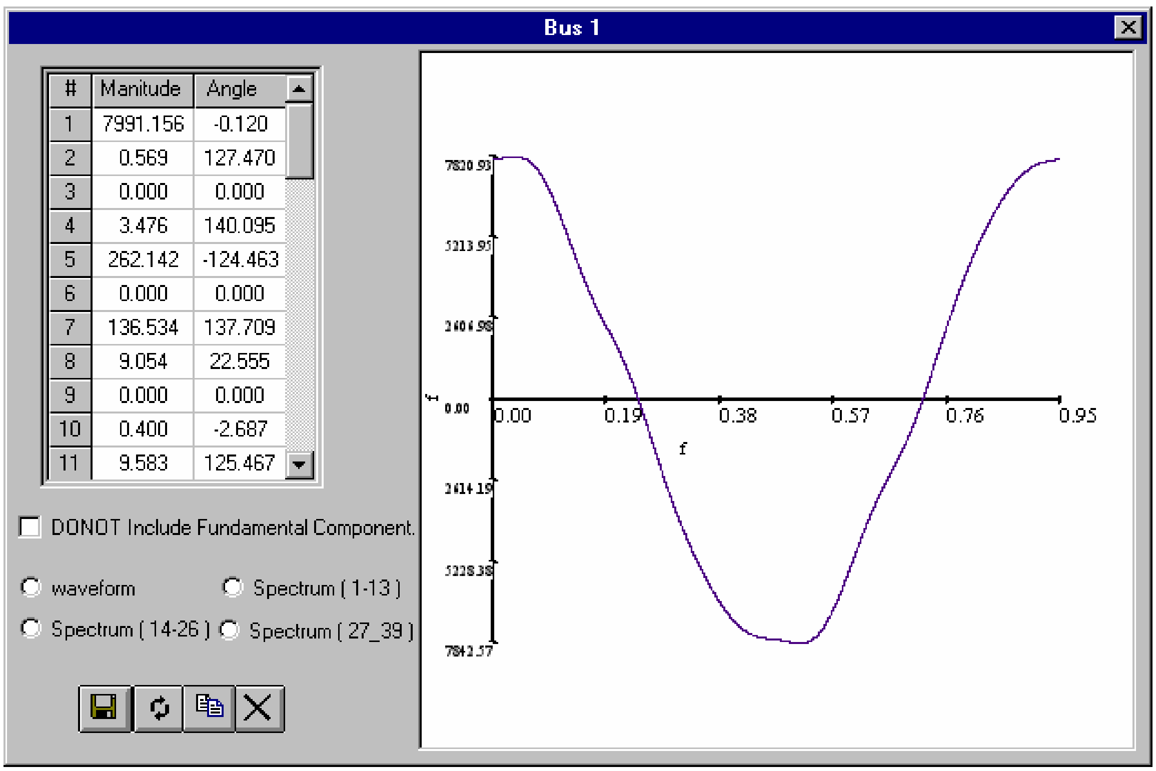

Figure 4.1. Dialog Box with Bus 1 Harmonic Voltage Data and Waveform.

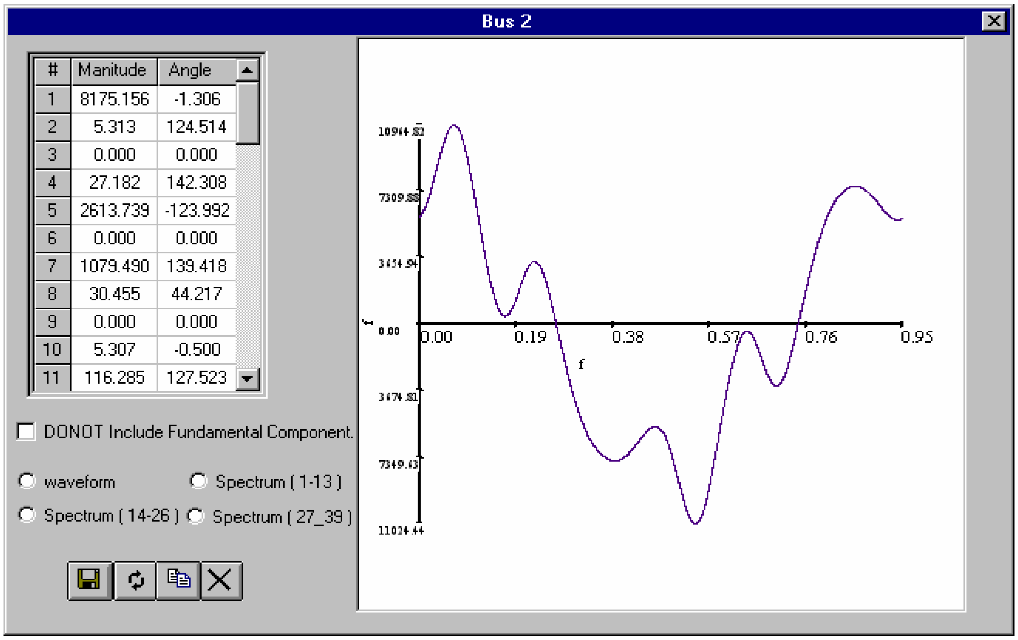

Figure 4.2. Dialog Box with Bus 2 Harmonic Voltage Data and Waveform

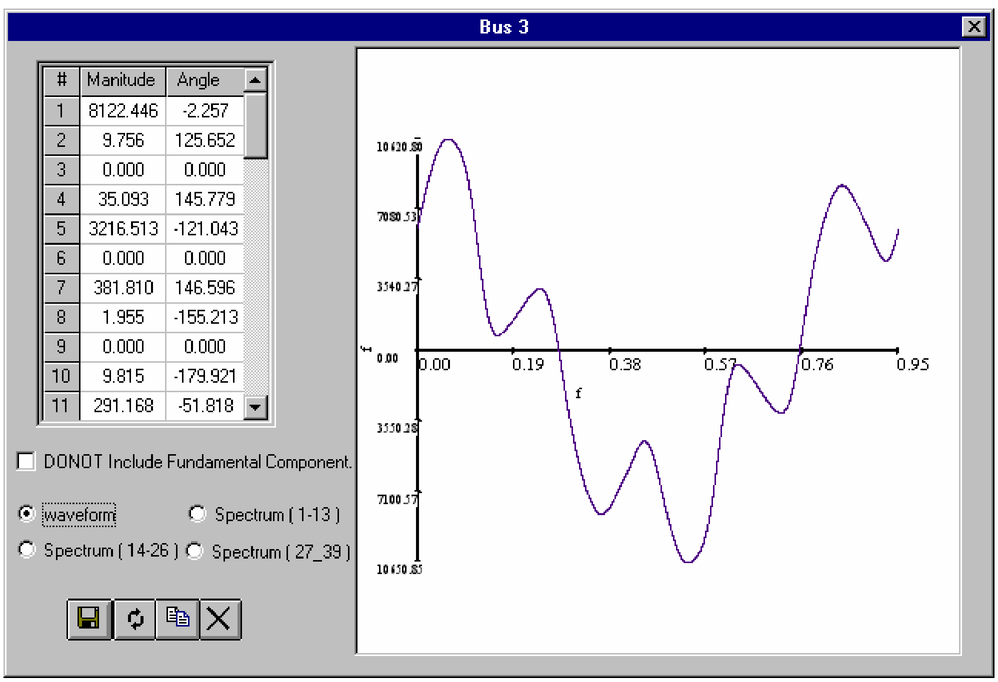

Figure 4.3. Dialog Box with Bus 3 Harmonic Voltage Data and Waveform

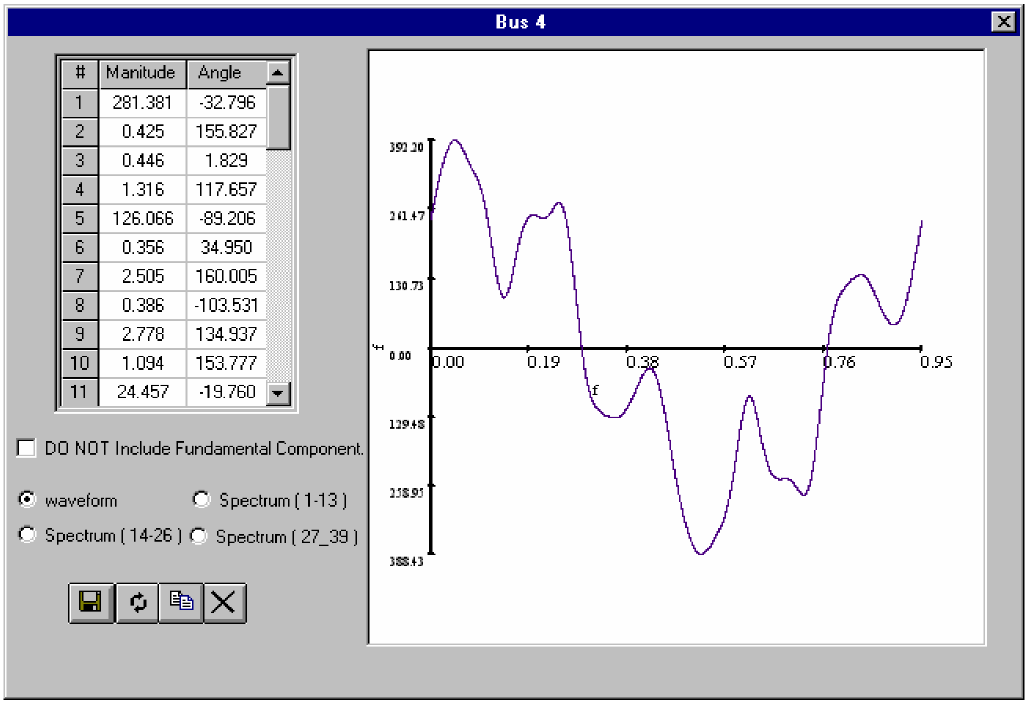

Figure 4.4. Dialog Box with Bus 4 Harmonic Voltage Data and Waveform

Comparing the voltage waveforms of Figures 4.1, 4.2, 4.3 and 4.4, it can be deduced that the bus voltages of buses 2, 3 and 4 are severely distorted as compared to bus 4. The huge voltage waveform deviation from the pure sinusoid at bus 4 is consistent with the numerical data of the voltage harmonics in the Tables 4.2 and 4.3. Because the nonlinear load is connected to bus 4 the voltage harmonics produced at bus 4 are greater as compared to other bus voltages.

The distorted voltage waveform provides a visual estimation of the potential effect of harmonic currents produced by the nonlinear loads used. Looking at the distorted voltage waveform, the user can make quick engineering decisions and analyses of possible harmonic problems. In Figures 4.1, 4.2, 4.3 and 4.4, the individual harmonic magnitudes and angles are displayed in the grid. This gives the user numerical data associated with the harmonic voltages. The numerical data can further be used to apply the IEEE 519 voltage harmonic limits.

The IEEE 519 standard suggests voltage harmonic limits for individual harmonics and for total harmonic distortion. Different limits are suggested for different voltage levels. Table 4.4 summarizes the IEEE 519 limits on voltage harmonics.

Table 4.4. IEEE 519 Harmonic Voltage Limits

Voltage at PCC	Individual limit	Total harmonic distortion
<69 kV	3.0	5.0
69 – 161 kV	1.5	2.5
>161 kV	1.0	1.5

Total harmonic distortion (THD) in the table indicates the amount of waveform distortion compared to a perfect sinusoid. The calculated THD for voltage at bus 4 (from Table 4.2) is 46%. According to the limits set by IEEE 519, the voltage THD limit for a bus voltage below 69 kV is 5.0%. Therefore, the harmonic voltages at bus 4 are above the limit. Preventive measures such as filters or reducing the nonlinear load capacity can then be theoretically studied. For studying the affects of reducing the nonlinear load capacity, the same procedure can be followed. At this time, the developed application can not evaluate harmonic filter applications.

Case 2:

Continuing on the same case system as in case 1, consider the following nonlinear loads:

Table 4.5. Nonlinear Load Data for Case 2.

Load 1 (6 pulse converter with capacitive smoothing)	1. Three phase kVA 25 kVA 2. Phase to phase voltage kV of 0.48 kV 3. Power factor (displacement factor) of 0.75 lag 4. Harmonic (h=1 to 50) current magnitudes in percentage of the fundamental and angle in degrees are in Table 3 of Appendix
Load 2 (6 pulse converter with capacitive smoothing and a series inductor of >3%)	1. Three phase kVA 25 kVA 2. Phase to phase voltage kV of 0.48 kV 3. Power factor (displacement factor) of 0.75 lag 4. Harmonic (h=1 to 50) current magnitudes in percentage of the fundamental and angle in degrees are in Table 4 of Appendix.

Notice that the capacity of the nonlinear loads is reduced as compared to case 1. The dialog box in Figure 4.5 is the AAC criteria applied to the nonlinear loads. When AAC is applied to the two nonlinear loads, the ratio of weighted capacity of the two loads to the short circuit capacity at the PCC (551kVA) is 13.6%. As compared to case 1, the amount by which the ratio exceeds the 0.1% limit of AAC is small (however the ratio exceeds the 0.1%). Therefore, it can be anticipated that the amount of voltage distortion will be less. Tables 4.6and 4.7 are the results for the bus voltage harmonics from the application developed and Superharm, respectively. In Tables 4.6 and 4.7 “Mag” is magnitude in volts, “Angle” is angle in degrees and “H#” is harmonic number.

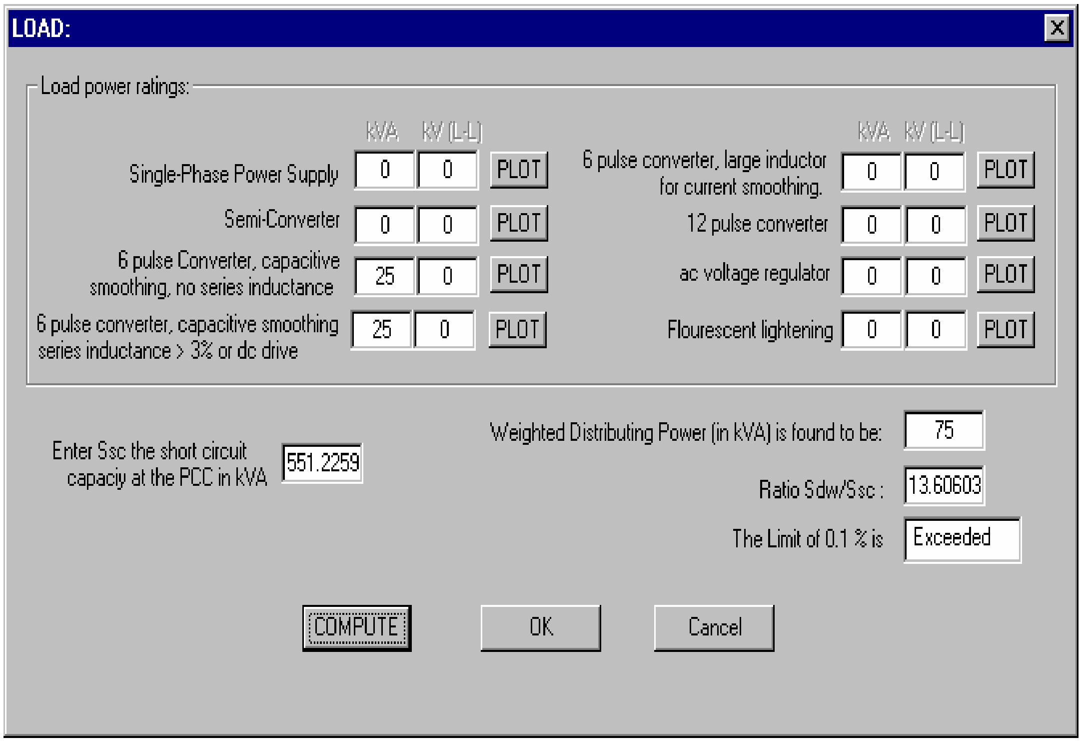

Figure 4.5. Dialog Box with the AAC Limit Verification.

Table 4.6. Results of the Sample Case 2 Using the Application.

H	Bus 1		Bus 2		Bus 3		Bus 4	
#	Mag	Angle	Mag	Angle	Mag	Angle	Mag	Angle
1	8005.61	-0.03	8324.79	-0.56	8407.39	-0.74	294.04	-30.87
2	0.06	132.62	0.55	129.13	1.01	129.85	0.04	159.69
3	0.00	0.00	0.00	0.00	0.00	0.00	0.05	7.62
4	0.24	155.93	2.29	154.18	3.35	155.18	0.14	125.38
5	31.61	-110.14	297.65	-111.54	349.37	-110.13	13.17	-79.55
6	0.00	0.00	0.00	0.00	0.00	0.00	0.04	46.54
7	9.79	157.25	92.11	156.25	36.68	161.52	0.26	173.53
8	0.17	68.32	1.64	67.44	0.16	-137.14	0.04	-88.08
9	0.00	0.00	0.00	0.00	0.00	0.00	0.29	152.32
10	0.14	25.70	1.30	25.00	1.63	-157.25	0.11	173.09
11	2.17	153.60	20.44	152.96	39.56	-28.63	2.56	1.49

Table 4.6 (continued)

H	Bus 1		Bus 2		Bus 3		Bus 4	
#	Mag	Angle	Mag	Angle	Mag	Angle	Mag	Angle
12	0.00	0.00	0.00	0.00	0.00	0.00	0.32	-152.01
13	0.77	58.30	7.25	57.77	25.28	-123.26	1.52	-153.27
14	0.00	-63.07	0.04	-63.57	0.16	115.55	0.01	145.52
15	0.00	0.00	0.00	0.00	0.00	0.00	0.33	81.75
16	0.00	-164.65	0.02	-165.08	0.15	14.22	0.01	-15.82
17	0.09	-120.60	0.89	-121.01	6.56	58.36	0.37	88.32
18	0.00	0.00	0.00	0.00	0.00	0.00	0.02	64.13
19	0.03	176.55	0.32	176.18	3.09	-4.35	0.17	-34.40
20	0.00	114.93	0.02	114.58	0.21	-65.92	0.01	-35.96
21	0.00	0.00	0.00	0.00	0.00	0.00	0.06	-159.62
22	0.00	128.26	0.01	127.95	0.18	-52.49	0.01	-82.53
23	0.00	164.52	0.04	164.22	0.59	-16.19	0.03	13.76
24	0.00	0.00	0.00	0.00	0.00	0.00	0.01	-120.87
25	0.00	116.31	0.03	116.03	0.56	-64.64	0.03	-94.38
26	0.00	-56.95	0.01	-57.22	0.14	122.43	0.01	152.39
27	0.00	0.00	0.00	0.00	0.00	0.00	0.02	59.51
28	0.00	-105.04	0.00	-105.29	0.04	74.39	0.00	44.35
29	0.00	-63.18	0.01	-63.42	0.31	116.27	0.02	146.23
30	0.00	0.00	0.00	0.00	0.00	0.00	0.00	69.21
31	0.00	152.80	0.02	152.57	0.48	-27.71	0.03	-57.75
32	0.00	176.01	0.00	175.79	0.04	-4.49	0.00	25.48
33	0.00	0.00	0.00	0.00	0.00	0.00	0.00	-125.40
34	0.00	126.13	0.00	129.92	0.05	-54.34	0.00	-84.37
35	0.00	-85.45	0.00	-85.65	0.10	94.10	0.01	124.07
36	0.00	0.00	0.00	0.00	0.00	0.00	0.00	178.66
37	0.00	48.78	0.01	48.59	0.24	-131.65	0.01	-161.67
38	0.00	-23.98	0.00	-24.17	0.04	155.60	0.00	-174.43
39	0.00	0.00	0.00	0.00	0.00	0.00	0.00	67.71
41	0.00	-94.28	0.00	-94.45	0.00	85.34	0.01	115.32
42	0.00	0.00	0.00	0.00	0.14	0.00	0.00	49.49
43	0.00	-104.29	0.00	-104.46	0.02	75.34	0.01	45.32
44	0.00	-169.20	0.00	-169.36	0.00	10.45	0.00	40.42
45	0.00	0.00	0.00	0.00	0.01	0.00	0.00	-159.90
46	0.00	77.73	0.00	77.58	0.01	-102.60	0.00	-132.63
47	0.00	145.82	0.00	145.67	0.05	-34.52	0.00	-4.54
49	0.00	177.07	0.00	176.92	0.06	-3.25	0.00	-33.27
50	0.00	-47.39	0.00	-45.53	0.03	132.30	0.00	162.27

Table 4.7. Results of the Sample Case 1 Using the Superharm.

H	Bus 1		Bus 2		Bus 3		Bus 4	
#	Mag	Angle	Mag	Angle	Mag	Angle	Mag	Angle
1	8004.95	-0.03	8318.52	-0.55	8395.16	-0.73	293.56	-30.85
2	0.05	132.66	0.54	129.17	1.01	129.89	0.04	159.73
3	0.00	-82.37	0.00	-84.70	0.00	-83.91	0.05	7.67
4	0.24	156.08	2.27	154.33	3.32	155.33	0.14	125.54
5	31.68	-110.02	298.33	-111.42	350.18	-110.01	13.21	-79.43
6	0.00	141.09	0.00	139.92	0.00	142.20	0.04	46.64
7	9.77	157.37	91.97	156.37	36.62	161.64	0.26	173.61
8	0.17	68.45	1.64	67.58	0.16	-137.00	0.04	-87.94
9	0.00	-130.91	0.00	-131.69	0.00	44.29	0.29	152.47
10	0.13	25.88	1.30	25.18	1.63	-157.08	0.11	173.27
11	2.16	153.78	20.42	153.15	39.52	-28.45	2.55	1.67
12	0.00	136.78	0.00	136.19	0.00	-45.05	0.32	-151.76
13	0.77	58.52	7.24	57.98	25.25	-123.05	1.52	-153.06
14	0.00	-62.84	0.04	-63.34	0.16	115.78	0.01	145.75
15	0.00	170.87	0.00	170.40	0.00	-10.37	0.37	80.95
16	0.00	-164.38	0.02	-164.82	0.15	14.49	0.01	-15.55
17	0.09	-107.72	0.85	-108.13	6.28	71.24	0.36	101.20
18	0.00	154.99	0.00	154.60	0.00	-25.97	0.02	64.42
19	0.03	176.86	0.32	176.49	3.09	-4.04	0.17	-34.09
20	0.00	115.26	0.02	114.91	0.21	-65.59	0.01	-35.63
21	0.00	-68.65	0.00	-68.98	0.00	110.55	0.06	-159.27
22	0.00	128.63	0.01	128.31	0.18	-52.12	0.01	-82.17
23	0.00	164.90	0.04	164.60	0.59	-15.81	0.03	14.14
24	0.00	-29.88	0.00	-30.17	0.00	149.44	0.01	-120.48
25	0.00	116.72	0.03	116.44	0.56	-63.93	0.03	-93.97
26	0.00	-56.52	0.01	-56.79	0.14	122.86	0.01	152.82
27	0.00	151.33	0.00	151.07	0.00	-29.27	0.02	60.78
28	0.00	-104.57	0.00	-104.82	0.04	74.85	0.00	44.82
29	0.00	-62.70	0.01	-62.94	0.31	116.75	0.02	146.71
30	0.00	160.22	0.00	159.98	0.00	-20.31	0.00	69.71
31	0.00	153.31	0.02	153.08	0.48	-27.20	0.03	-57.24
32	0.00	176.54	0.00	176.32	0.04	-3.96	0.00	26.01
33	0.00	-34.39	0.00	-34.60	0.00	145.13	0.00	-124.86
34	0.00	126.69	0.00	126.48	0.05	-53.77	0.00	-83.81
35	0.00	-84.87	0.00	-85.07	0.10	94.68	0.01	124.65

Table 4.7 (continued)

H #	Bus 1		Bus 2		Bus 3		Bus 4	
	Mag	Angle	Mag	Angle	Mag	Angle	Mag	Angle
36	0.00	-90.31	0.00	-90.51	0.00	89.25	0.00	179.25
37	0.00	49.39	0.01	49.20	0.24	-131.03	0.01	-161.06
38	0.00	-23.36	0.00	-23.54	0.04	156.23	0.00	-173.80
39	0.00	158.76	0.00	158.58	0.00	-21.64	0.00	68.36
41	0.00	-93.60	0.00	-93.77	0.10	86.02	0.01	116.00
42	0.00	140.57	0.00	140.40	0.00	-39.81	0.00	50.19
43	0.00	-103.58	0.00	-103.75	0.14	76.06	0.01	46.03
44	0.00	-168.47	0.00	-168.63	0.02	11.18	0.00	41.15
45	0.00	-68.80	0.00	-68.96	0.00	110.85	0.00	-159.16
46	0.00	78.50	0.00	78.34	0.01	-101.84	0.00	-131.87
47	0.00	146.59	0.00	146.44	0.05	-33.74	0.00	-3.76
49	0.00	177.88	0.00	177.73	0.06	-2.44	0.00	-32.46
50	0.00	-46.57	0.00	-46.71	0.03	133.12	0.00	163.10

When the user clicks on any bus, the dialog boxes with the harmonic voltages (voltage harmonic magnitudes and angles equal to data in Table 4.6) at that bus pops up. Figures 4.6, 4.7, 4.8 and 4.9 are the dialog boxes with the harmonic voltage data and the associated waveforms for buses 1, 2, 3 and 4, respectively.

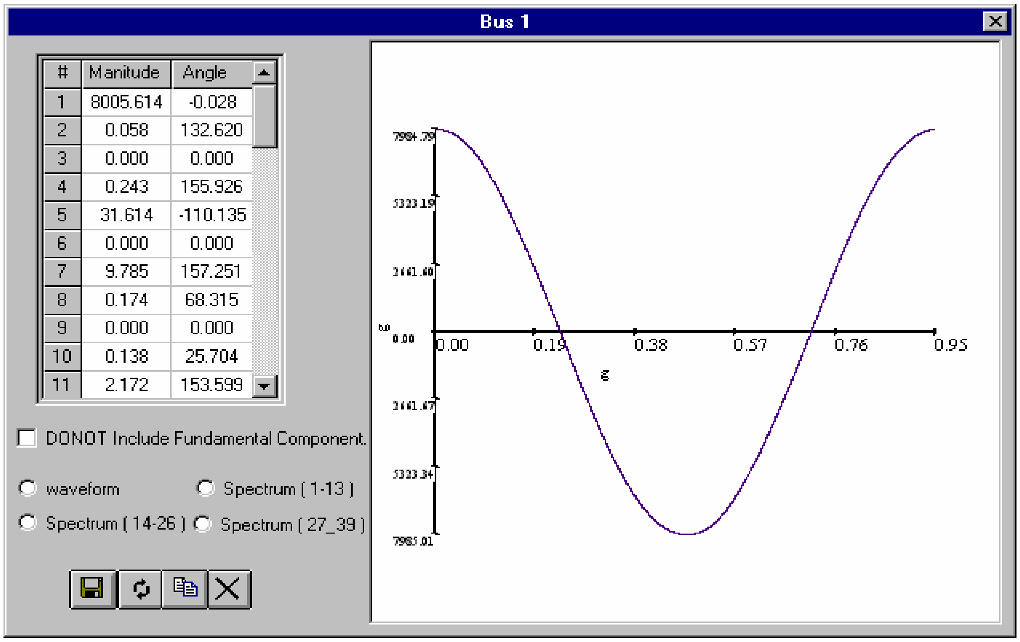

Figure 4.6. Dialog Box with Bus 1 Voltage.

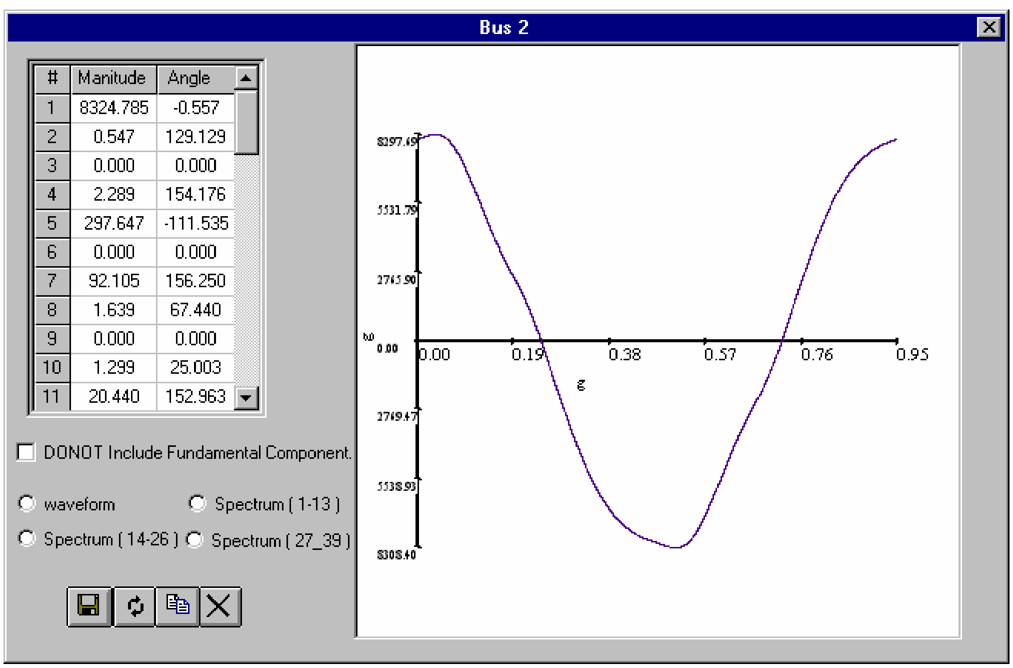

Figure 4.7. Dialog Box with Bus 2 Voltage.

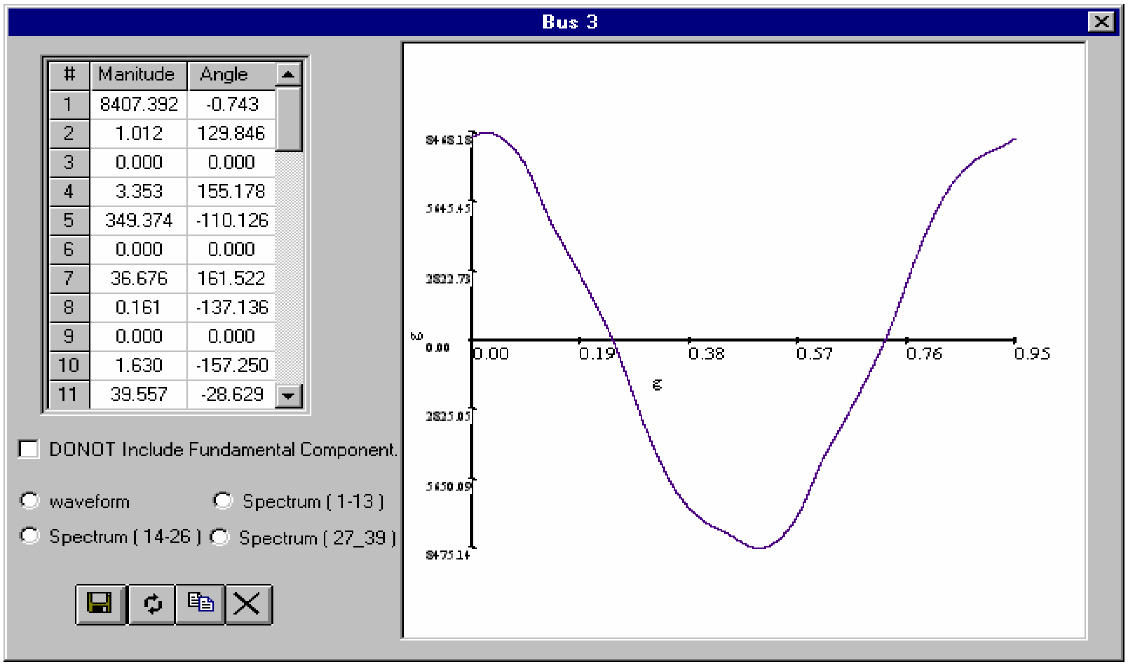

Figure 4.8. Dialog Box with Bus 3 Voltage.

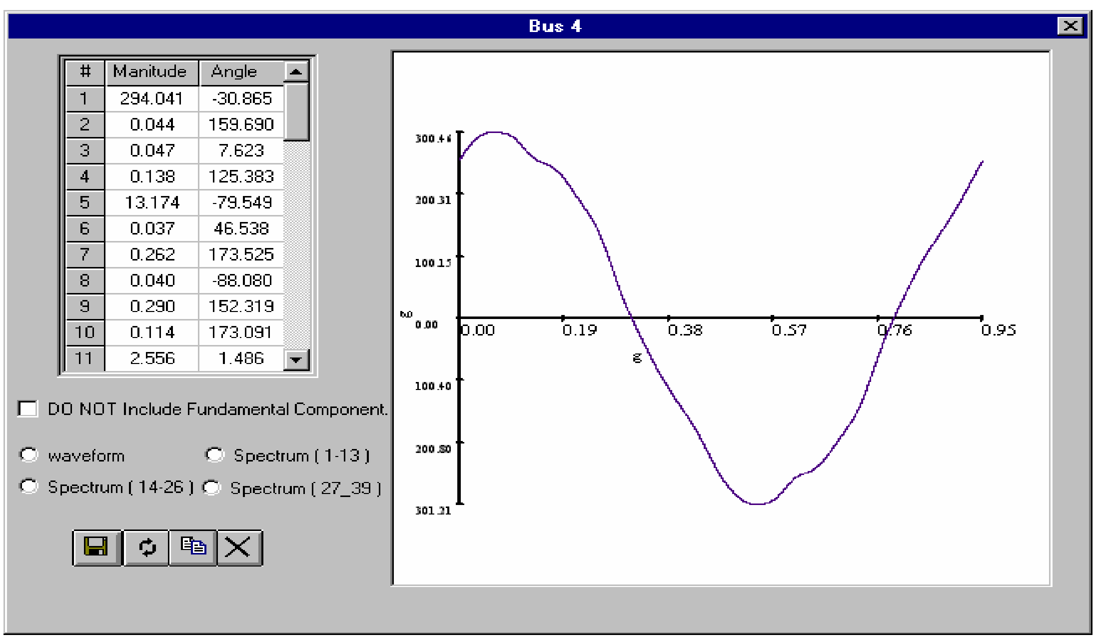

Figure 4.9. Dialog Box with Bus 4 Voltage.

Comparing the voltage waveform from case 1 and case 2, the distortions in the waveform for case 2 are less as anticipated. Therefore the application program developed as a part of the thesis gives theoretically anticipated results. To compare the computational accuracy the application program results were compared with Superharm simulation results.

Application Results' Validity

For the sample cases 1 and 2, the results generated by the program differ from Superharm results with a maximum margin of 10 volts in a 13800 volts system. The 10 volts difference is very negligible in such high voltage system. Therefore, it can be concluded that Superharm results confirm the accuracy of the application results. However, the in-built program of Superharm could have some inherent assumptions and/or there could be specific cases to which Superharm would not compute accurate results. Since the accuracy of the application program developed is evaluated based on Superharm simulated results, any assumptions in modeling of the network and in the implementation of the analytical approaches also apply to the application program developed. Superharm and the application program may have similar physics based flaws. Therefore the applicability of the program to any power system is limited by the assumptions and any in-built errors of Superharm as described in the Superharm's benchmarking guide [1].

CHAPTER V

CONCLUSION

An application program that estimates possible harmonic problems due to an existing or a proposed set of nonlinear loads was developed in this thesis work. The application was built to find the system response for multiple harmonic sources. The application included several user-interface features to facilitate the use of the application in the Windows environment.

The main feature of the application program is the presentation of the data. The numerical data and the graphical representation of the data help the user in having complete information about the harmonics present. The application gives the user means to document the results of a harmonic study with ease. The user can use the Windows copy-pasting commands for copying the harmonic numerical data from the application into a Microsoft Excel spreadsheet. The user can also document the harmonic waveform or spectral diagrams in the application in a Microsoft Word document by using the copy button available at the bottom left corner of the dialog boxes.

Apart from the user-interface advantages discussed in the previous paragraph, the application also offers several other advantages. The typical harmonic current characteristics of several common nonlinear loads are internally available in the application making it possible to perform harmonic analysis even in the absence of measured data. The application also gives the user the ability to modify the default data in case the actual data (measured or supplied by manufacturers) is different. The ease of using the application is another advantage of the application.

The user operates in the application environment without difficulty. The user is likely to find the application easy to use and to navigate through because of the simplicity of the user-interface feature of the application. The application can be installed on a computer by downloading the executable file of the application. All the controls used in the application are made available through the release mode of the application in the executable file. Microsoft Visual C++ software is not necessary for the application executable file to be used; only the Windows environment is required on the computer. This makes the application a memory space, time and cost efficient application as compared with many other harmonic analysis applications available.

Because the built-in system topology is representative of many power distribution systems (from a harmonic prospective), power engineers can use the application developed to perform harmonic analysis. The application can also be used as an educational simulation tool for beginners in power engineering to understand harmonics and harmonic impacts on the power system. However, it should be noted the application's accuracy is limited by the in-built assumptions of Superharm outlined in the Superharm benchmarking manual [1]. Other than the power engineering field, the application's basic Microsoft Visual C++ features like the grid can be used to develop other engineering applications.

Future Work

The developed application can be further expanded for harmonic current compliance with the IEEE harmonic current limits. The nonlinear load models can be further enhanced in detail to give the user the ability to simulate harmonic currents for different characteristics of loads (like firing angles for controlled rectifiers). Provisions can also be made internally such that the application verifies different harmonic bus voltages and harmonic branch currents for IEEE 519 limit compliance and displays such messages. Several other user interface features can be added to the application using Microsoft Visual C++. For example, a drawing feature could be added such that the user can construct a system and single line diagram of arbitrary complexity so that more advanced power systems can be studied.

References

[1] Electrotek Concepts, Inc, "SuperHarm Benchmarking Manual," October 15, 1998.

[2] Roger C. Dugan, Mark F. McGranaghan and H. Wayne Beaty, Electrical Power Systems Quality, McGraw-Hill, New York, 1996.

[3] Heydt, G. T., Computer Analysis Methods for Power Systems, Stars in a Circle Publications, Arizona, 1996.

[4] Thomas Grebe, Rory Dwyer and Afroz Khan, "HarmFlo+ Case Study Workbook In-house Training Edition," Electrotek Concepts, Inc., 1994.

[5] Heydt, G. T., Electric power Quality, Stars in a Circle Publications, Indiana, 1991.

[6] HarmFlo User's Group, "Harmonic Analysis using the HarmFlo+ Workstation," Electrotek Concepts, Inc., 1993.

[7] Duncan J. Glover and Mulukutla Sarma, Power System Analysis and Design, PWS Publishing Company, Boston, 1994.

[8] David J. Kruglinsky, George Shepherd and Scot Wingo, Programming Microsoft Visual C++, 5th Edition, Microsoft Press, 1998.

[9] Chris Maunder, "Grid Control in a view," Code project, http://www.codeproject. com/miscctrl/grid-in-views.asp.

[10] Ned Mohan, Tore M. Undeland and William P. Robbins, Power Electronics – Converters, Applications and Design, 2nd Edition, John Wiley & Sons, Inc., New York, 1989.

[11] Bimbhra, P. S., Power Electronics, 1st Edition, Khanna Publishers, Delhi, 1997.

APPENDIX

Single-phase Power Supply

The harmonic spectrum data for the single-phase power supply was obtained from a measured case given in the Superharm manual. In Figure A1 the simple circuit [10] of a single-phase power supply is shown. Table A1 contains the typical harmonic data for the single-phase supply load. In Table A1 “Mag” is the percentage magnitude and “Ang” is the angle in degrees.

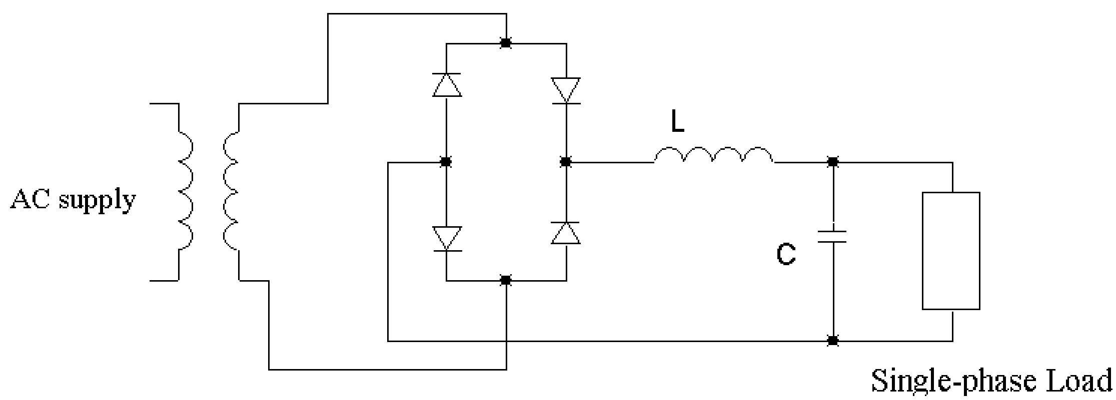

Figure A1. Single-phase Power Supply.

Table A1. Harmonic Spectrum for Single-phase Power Supply Load.

Harmonic#	Mag(%)	Ang(deg)
1	100.0000	-37.0000
2	0.0000	90.0000
3	65.7000	83.0000
4	0.0000	270.0000
5	37.7000	194.0000
6	0.0000	90.0000

Table A1 (continued)

Harmonic#	Mag(%)	Ang(deg)
7	12.7000	293.0000
8	0.0000	270.0000
9	4.4000	314.0000
10	0.0000	90.0000
11	5.3000	22.0000
12	0.0000	270.0000
13	2.5000	92.0000
14	0.0000	90.0000
15	1.9000	129.0000
16	0.0000	270.0000
17	1.8000	209.0000
18	0.0000	90.0000
19	1.1000	264.0000
20	0.0000	270.0000
21	0.6000	319.0000
22	0.0000	90.0000
23	0.0000	180.0000
24	0.0000	270.0000
25	0.0000	0.0000
26	0.0000	90.0000
27	0.2000	180.0000
28	0.0000	270.0000
29	0.2000	0.0000
30	0.0000	90.0000
31	0.2000	180.0000
32	0.0000	270.0000
33	0.2000	0.0000

Semi-converter

A single-phase semi-converter bridge [10] with two thyristors (X1, X2) and two diodes (D1, D2) is in Figure A2. In Figure A2, L1 was 5 mH, C1 was 0.01 mF and R1 was 15 ohms. The thyristers X1 and X2 were fired at an angle of 30 degrees and the supply source voltage VA was 339 V at 0°. In order to obtain the spectral results via simulation, the components in the circuit in Figure A2 require having the values stated previously. The harmonic current data for the semi-converter is in Table A2. In Table A2 "Mag" is the percentage magnitude and "Ang" is the angle in degrees.

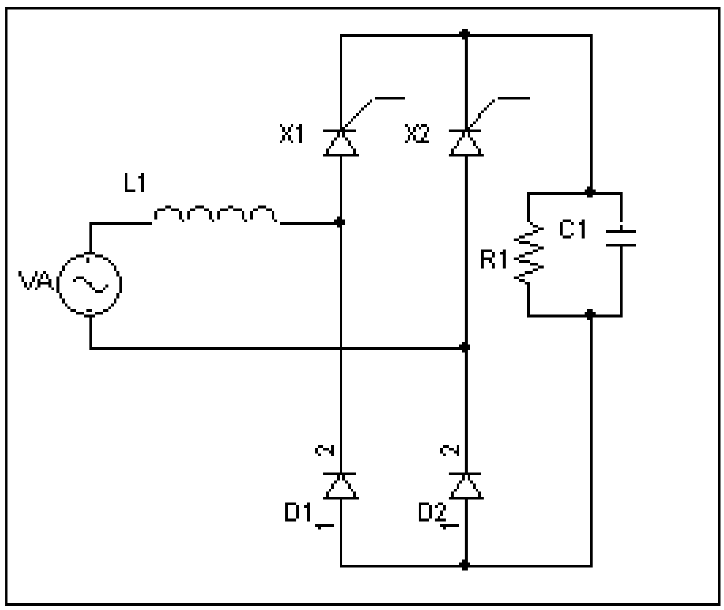

Figure A2. Semi-converter.

Table A2. Spectrum for Semi-converter.

Harmonic#	Mag(%)	Ang(deg)
1	100.0000	58.0400
2	0.0050	-56.8100
3	8.3920	35.6500
4	0.0050	-23.7900
5	7.5600	117.1000

Table A2 (continued)

Harmonic#	Mag(%)	Ang(deg)
6	0.0050	9.0810
7	6.1310	-164.9000
8	0.0050	45.0800
9	4.3300	-89.9400
10	0.0050	80.9700
11	2.6650	-18.8200
13	1.5330	43.7600
14	0.0040	141.9000
15	1.0540	95.9800
16	0.0030	171.7000
17	0.9660	155.3000
18	0.0020	-147.6000
19	0.9100	-131.8000
20	0.0010	-86.5800
21	0.7820	-52.2300
22	0.0010	-7.0190
23	0.6030	28.5600
24	0.0010	58.5100
25	0.4200	105.6000
26	0.0010	97.0700

6 Pulse Converter

A 6-pulse converter is often called a three-phase full converter. In Figure A3 one of the applications of a 6-pulse converter is shown. The typical configuration in Figure A3 is called a 6 pulse converter with capacitive smoothing on the dc side [10]. The harmonic current data for a 6 pulse converter with capacitive smoothing (on the dc side) is in Table A3. The data in Table A3 were collected from the simulated case study in the

Superharm manual. In Table A3 “Mag” is the percentage magnitude and “Ang” is the angle in degrees.

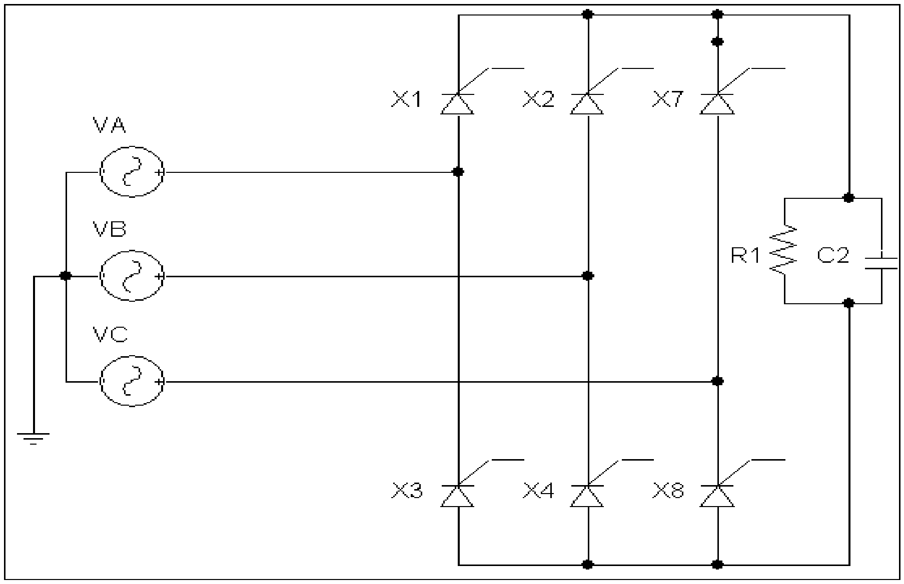

Figure A3. 6 Pulse Converter with Capacitive Smoothing.

Table A3. Harmonic Current Spectrum of 6 Pulse Converter with Capacitive Smoothing.

Harmonic#	Mag(%)	Ang(deg)
1	100.0000	10.0000
2	1.1000	78.0000
3	3.9000	-122.0000
4	0.5000	167.0000
5	82.8000	-125.0000
6	1.7000	-56.0000
7	77.5000	79.0000
8	1.2000	131.0000
9	7.6000	-80.0000
10	0.7000	112.0000
11	46.3000	-52.0000
12	1.0000	-48.0000
13	41.2000	149.0000

Table A3 (continued)

Harmonic#	Mag(%)	Ang(deg)
14	0.0000	0.0000
15	5.7000	-26.0000
16	0.3000	172.0000
17	14.2000	19.0000
18	0.4000	78.0000
19	9.7000	-145.0000
20	0.4000	-138.0000
21	2.3000	19.0000
22	0.5000	-14.0000
23	1.5000	-148.0000
24	0.5000	89.0000
25	2.5000	108.0000
26	0.7000	-135.0000
27	0.9000	-29.0000
28	0.3000	9.0000
29	2.0000	-29.0000
30	0.2000	55.0000
31	2.0000	169.0000
32	0.3000	149.0000
33	0.5000	-19.0000
34	0.4000	-61.0000
35	0.3000	-147.0000
36	0.1000	25.0000
37	0.8000	75.0000
38	0.3000	148.0000
39	0.5000	-58.0000
40	0.0000	0.0000
41	0.6000	-100.0000
42	0.0000	0.0000
43	0.7000	114.0000
44	0.1000	113.0000
45	0.4000	-59.0000
46	0.1000	-32.0000
47	0.2000	165.0000
48	0.0000	0.0000
49	0.4000	44.0000
50	0.3000	144.0000

A typical 6-pulse converter with capacitive smoothing on the dc side [10] is shown in Figure A4. The harmonic current data for a 6 pulse converter with capacitive smoothing (on the dc side) is in Table A4. The data in Table A4 were collected from the simulated case study in Superharm manual. In Table A4 "Mag" is the percentage magnitude and "Ang" is the angle in degrees.

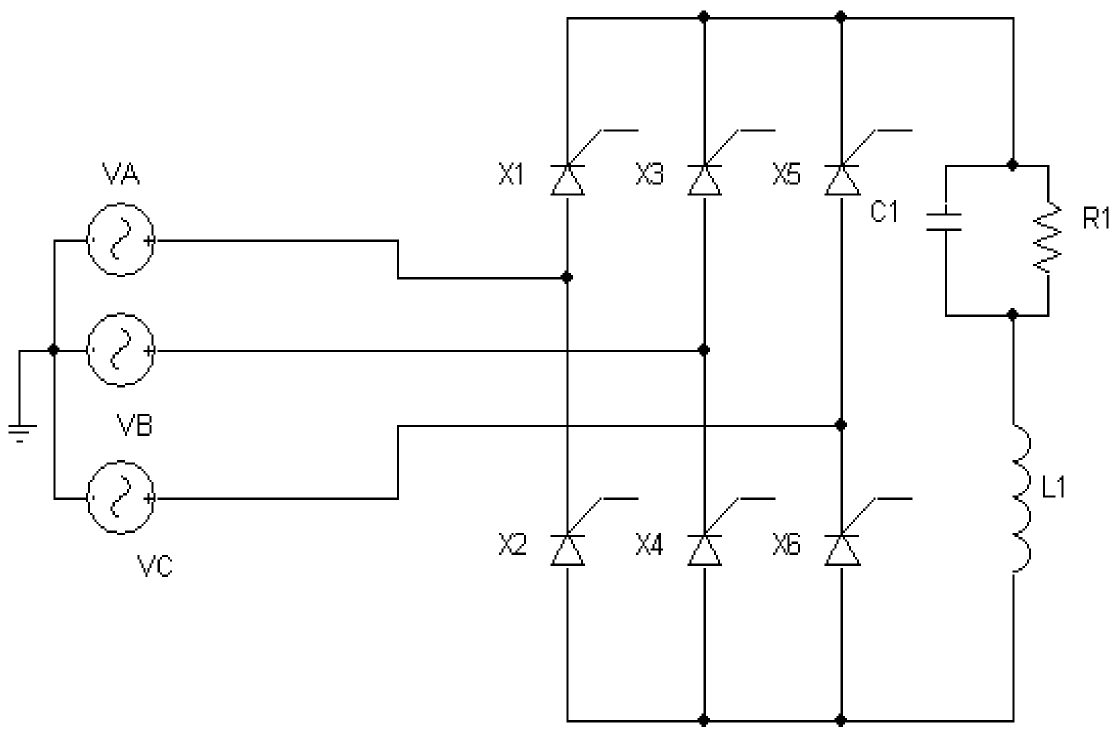

Figure A4. 6 Pulse Converter with Series Capacitor and Inductor.

Table A4. Harmonic Spectrum of 6 Pulse Converter with Series Capacitor and Inductor

Harmonic#	Mag(%)	Ang(deg)
1	100.0000	-128.0000
2	1.0000	145.0000
3	3.9000	-149.0000
4	0.4000	-57.0000
5	39.7000	-122.0000
6	0.8000	175.0000
7	18.9000	122.0000
8	0.2000	10.0000
9	0.8000	47.0000
10	0.2000	159.0000
11	6.8000	67.0000
12	0.4000	-27.0000
13	3.8000	-118.0000
14	0.3000	111.0000
15	0.4000	-140.0000
16	0.4000	6.0000
17	3.2000	-144.0000
18	0.4000	109.0000
19	2.3000	10.0000
20	0.3000	2.0000
21	0.3000	29.0000
22	0.2000	141.0000
23	1.8000	11.0000
24	0.2000	-79.0000
25	1.7000	145.0000
26	0.2000	124.0000
27	0.2000	-165.0000
28	0.1000	-81.0000
29	1.1000	160.0000
30	0.1000	68.0000
31	1.3000	-74.0000
32	0.1000	-112.0000
33	0.2000	-32.0000
34	0.1000	81.0000
35	0.7000	-49.0000
36	0.1000	-114.0000
37	1.0000	67.0000

Table A4 (continued)

Harmonic#	Mag(%)	Ang(deg)
38	0.0000	0.0000
39	0.2000	153.0000
40	0.0000	0.0000
41	0.5000	96.0000
42	0.1000	-1.0000
43	0.8000	-147.0000
44	0.1000	134.0000
45	0.2000	-59.0000
46	0.0000	0.0000
47	0.4000	-112.0000
48	0.0000	0.0000
49	0.7000	-5.0000
50	0.0000	0.0000

A 6-pulse converter with large inductor on the dc side for current smoothing [10] is shown in Figure A5. In Table A5 the harmonic current spectrum data of 6 pulse converter with a large inductor on the dc side are summarized. The circuit in Figure A5 was simulated in Pspice and the first 25 harmonics were obtained. In the circuit of Figure A5, L1, L2 and L3 were each 0.4mH, R1 was 2Ω and L4 was 2mH. The thyristors were fired at a firing angle of 30 degrees. In order to obtain the spectral results via simulation, the components in the circuit in Figure A5 require having the values stated previously. The supply source was a balanced three-phase supply of 169.7 L-L volts. In Table A5 "Mag" is the percentage magnitude and "Ang" is the angle in degrees.

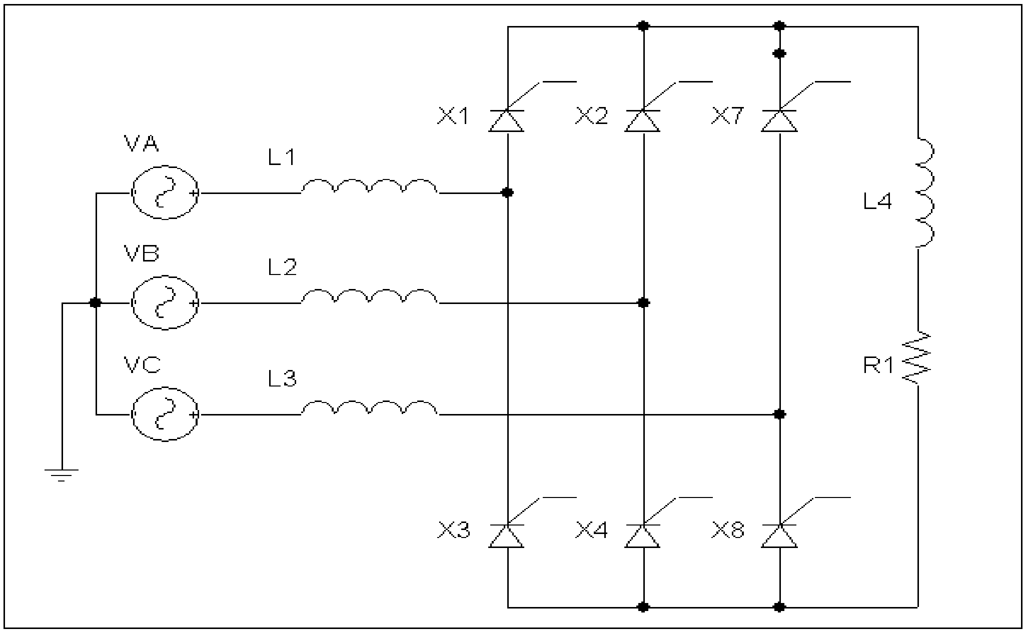

Figure A5. 6 Pulse Converter with Large Inductor.

Table A5. Harmonic Spectrum of 6 Pulse Converter with Large Inductor.

Harmonic#	Mag(%)	Ang(deg)
1	100.0000	24.5200
2	0.0055	-38.5300
3	0.0023	-132.6000
4	0.0046	37.0600
5	22.4500	-57.6800
6	0.0005	71.8400
7	9.9200	-9.8590
8	0.0124	-68.1800
9	0.0019	-153.7000
10	0.0107	-15.4700
11	7.3090	-92.7800
12	0.0006	30.0500
13	5.0090	-43.0800
14	0.0147	-104.1000

Table A5 (continued)

Harmonic#	Mag(%)	Ang(deg)
15	0.0014	166.7000
16	0.0153	-50.0200
17	3.3030	-128.1000
18	0.0005	10.4100
19	2.6500	-77.7200
20	0.0128	-135.0000
21	0.0008	133.6000
22	0.0150	-85.7600
23	1.3940	-165.6000
24	0.0005	-24.5700
25	1.2400	-114.1000

12 Pulse Converter

Figure A6 is the 12 pulse converter Pspice simulation schematic diagram. Two three-phase transformers were used in the circuit. Each of the two transfomers was built using three two winding transformers. One of the two three phase transfomers was Δ-Y connected and the other Y-Y connected. It was observed that the waveform distortions in the secondary side ac line current were smoothed on the primary side making the primary line current a perfect sinusoid. To have the distortions transferred to the primary line current, voltage dependent current sources were used. Two dummy voltage sources of 0 volts each were placed in line (a-phase) on each of the secondaries of the three phase transformers. A voltage dependent current source (curent depending on the voltage across the dummy voltage source on a-phase were connected in parallel to load. The subcircuit in Figure A6 is for the voltage dependent current source circuit. In Table A6 the harmonic current spectra of the 12 pulse converter is summarized. In Table A6 “Mag” is the percentage magnitude and “Ang” is the angle in degrees.

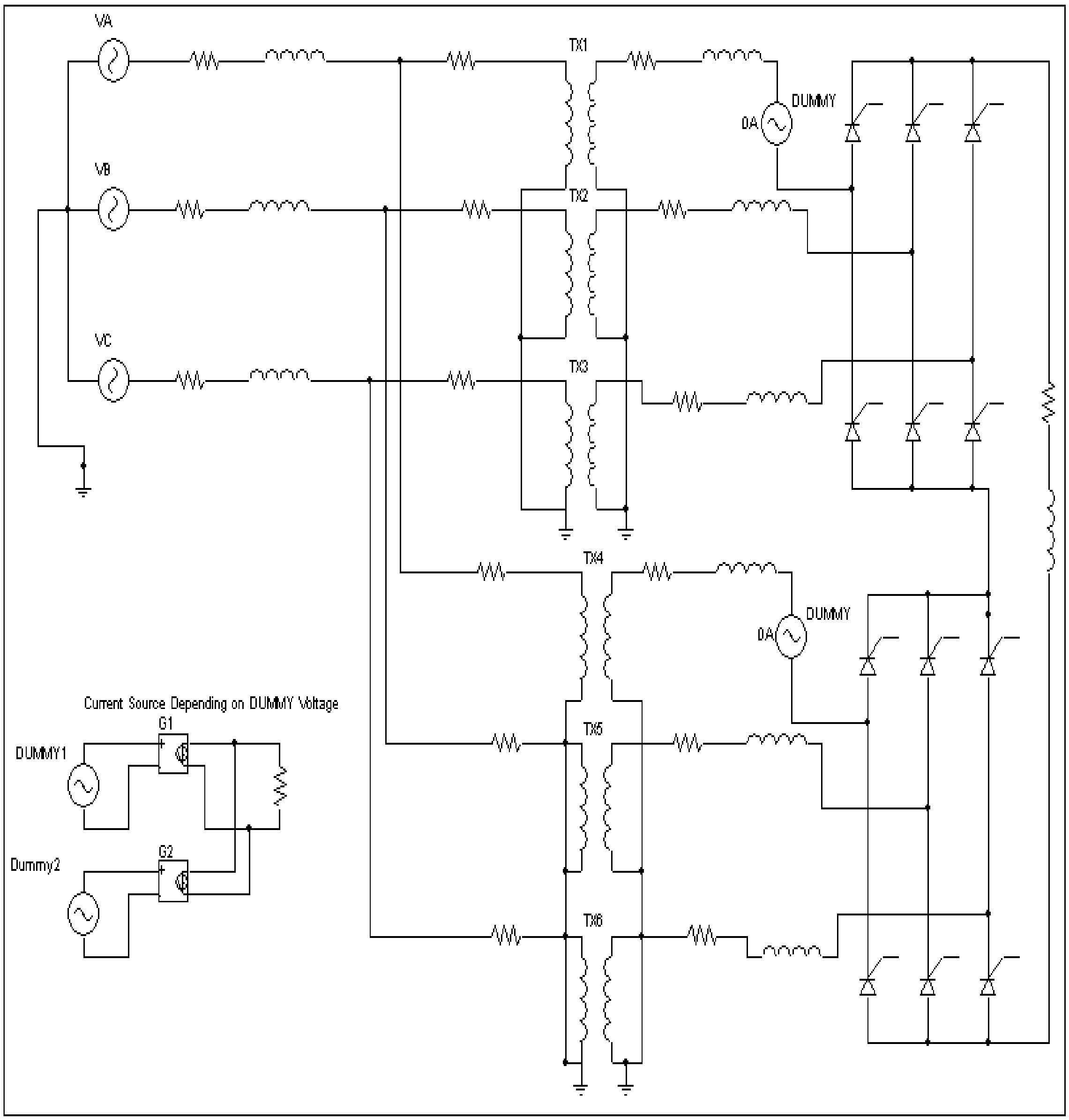

Figure A6. 12 Pulse Converter with Series Resistor and Inductor.

Table A6. Harmonic Current Spectrum of 12 Pulse Converter.

Harmonic#	Mag(%)	Ang(deg)
1	100.0000	-29.1300
2	0.3360	95.2700
3	0.1490	172.7000
4	0.3330	45.5500
5	0.6780	87.6400
6	0.2390	-30.3100
7	0.7030	-70.6700
8	1.1390	15.1100
9	1.5750	-167.6000
10	0.8000	0.9800
11	1.6670	121.9000
12	0.7910	-62.8600
13	1.7840	-13.2300
14	0.8870	-76.5300
15	2.6140	-114.2000
16	0.4530	-93.4100
17	0.2840	-103.7000
18	0.5340	-83.3800
19	1.5110	-116.9000
20	0.2050	31.6200
21	0.7330	135.2000
22	0.0830	-69.5400
23	0.4740	4.4410
24	0.2510	69.2500
25	0.2390	-98.5400

AC Voltage Regulator

An AC voltage regulator is another one of the nonlinear loads provided for use. A single phase ac voltage regulator [11] with a resistive load is in Figure A7. Table A7 contains the typical harmonic current data for the ac voltage regulator. In Table A7 “Mag” is the percentage magnitude and “Ang” is the angle in degrees.

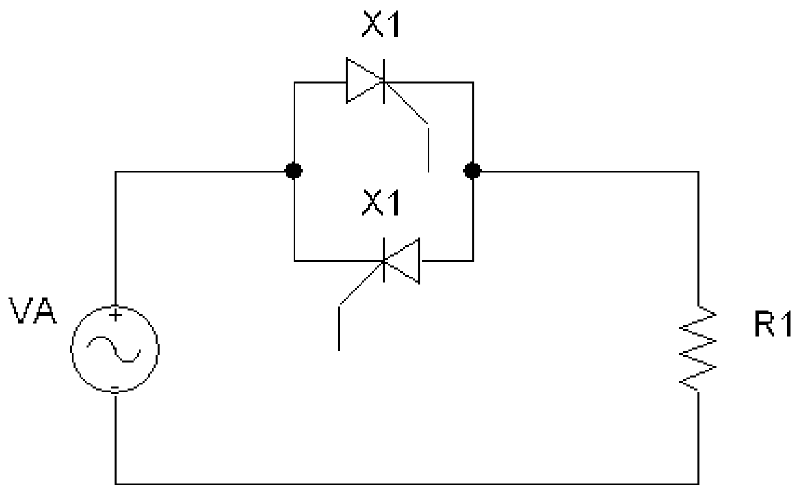

Figure A7. Single-phase AC Voltage Regulator

Table A7. Harmonic Current Spectrum for AC Voltage Regulator.

Harmonic#	Mag(%)	Ang(deg)
1	100.0000	58.0400
2	0.0050	-56.8100
3	8.3920	35.6500
4	0.0050	-23.7900
5	7.5600	117.1000
6	0.0050	9.0810
7	6.1310	-164.9000
8	0.0050	45.0800
9	4.3300	-89.9400
10	0.0050	80.9700
11	2.6650	-18.8200
12	0.0040	113.5000
13	1.5330	43.7600
14	0.0040	141.9000
15	1.0540	95.9800
16	0.0030	171.7000

Table A7 (continued)

Harmonic#	Mag(%)	Ang(deg)
17	0.9660	155.3000
18	0.0020	-147.6000
19	0.9100	-131.8000
20	0.0010	-86.5800
21	0.7820	-52.2300
22	0.0010	-7.0190
23	0.6030	28.5600
24	0.0010	58.5100
25	0.4200	105.6000
26	0.0010	97.0700

Fluorescent Lighting

Fluorescent lighting is a form of electric lighting that is very commonly used in commercial and residential applications. Figure A8 is the three-phase fluorescent lamp connection [5]. In Table A8 "Mag" is the percentage magnitude and "Ang" is the angle in degrees.

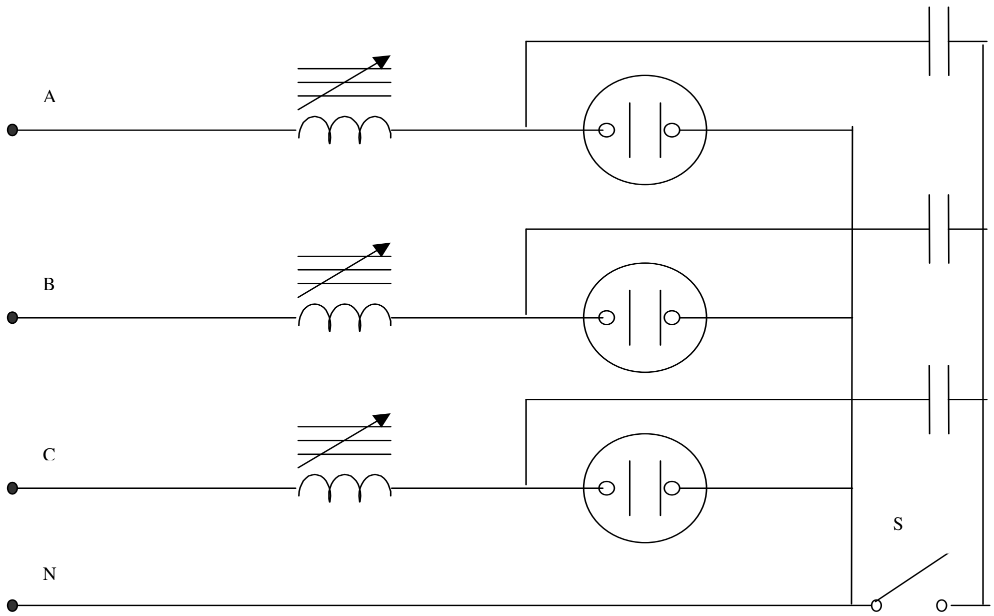

Figure A8. Fluorescent Lamp.

Table A8. Harmonic Current Spectrum for Fluorescent Lamp.

Harmonic#	Mag(%)	Ang(deg)
1	100.0000	0.0000
2	1.0000	92.3200
3	12.5930	-39.0980
4	0.3200	0.0260
5	1.8290	148.3160
6	0.0730	-166.8840
7	0.6800	-11.3840
8	0.0670	-62.6780
9	0.4680	-165.5700
10	0.1050	-149.0600
11	0.1920	-0.8790
12	0.0900	72.1000
13	0.1980	170.7930
14	0.0450	56.6500
15	0.0930	-52.9640

Table A8. (continued)

Harmonic#	Mag(%)	Ang(deg)
16	0.0860	-74.2070
17	0.1810	142.9300
18	0.0790	138.9810
19	0.0770	-63.3530
20	0.1500	-85.1520
21	0.1620	163.2340
22	0.0860	173.9200
23	0.0870	-53.8860
24	0.0410	-82.8850
25	0.1060	169.4600
26	0.0240	-115.8250
27	0.0770	-42.9620
28	0.0760	41.3620
29	0.1210	-155.4170
30	0.0570	-154.8870
31	0.0390	-102.3620
32	0.0730	-51.4650
33	0.0600	63.4480
34	0.0730	-26.0820
35	0.1020	-43.7960
36	0.0990	29.1490
37	0.0330	101.9540
38	0.0260	-75.7240
39	0.1070	-8.6500
40	0.1090	20.8660
41	0.1110	140.9510
42	0.0910	-9.6240
43	0.1170	174.8180
44	0.0700	77.2510
45	0.1070	142.0000
46	0.0730	13.5940
47	0.0910	-153.8980
48	0.0380	-14.6130
49	0.1180	133.7560